IEEE Access
Multidisciplinary | Rapid Review | Open Access Journal

Received January 18, 2021, accepted February 15, 2021, date of publication February 18, 2021, date of current version March 2, 2021.

Digital Object Identifier 10.1109/ACCESS.2021.3060031

Optimal Planning and EMS Design of PV Based Standalone Rural Microgrids

HABIB UR RAHMAN HABIB[1,2], (Member, IEEE), ASAD WAQAR[3], ABDUL KHALIQUE JUNEJO[1,4], MAHMOUD F. ELMORSHEDY[5], (Member, IEEE), SHAORONG WANG[1], MAHMUT SAMI BÜKER[6], KAYODE TIMOTHY AKINDEJI[7], (Member, IEEE), JEUK KANG[8], AND YUN-SU KIM[8], (Member, IEEE)

[1]State Key Laboratory of Advanced Electromagnetic Engineering and Technology, School of Electrical and Electronic Engineering, Huazhong University of Science and Technology, Wuhan 430074, China
[2]Department of Electrical Engineering, Faculty of Electrical and Electronics Engineering, University of Engineering and Technology Taxila, Taxila 47050, Pakistan
[3]Department of Electrical Engineering, Bahria University, Islamabad 44000, Pakistan
[4]Department of Electrical Engineering, Qaid-e-Awam University of Engineering, Science and Technology, Nawabshah 67450, Pakistan
[5]Electrical Power and Machines Engineering Department, Faculty of Engineering, Tanta University, Tanta 31512, Egypt
[6]Department of Aeronautical Engineering, NEU University, 42140 Konya, Turkey
[7]Department of Electrical Power Engineering, Faculty of Engineering and the Built Environment, Durban University of Technology, Durban 4000, South Africa
[8]Graduate School of Energy Convergence, Gwangju Institute of Science and Technology (GIST), Gwangju 61005, South Korea

Corresponding author: Yun-Su Kim (yunsukim@gist.ac.kr)

This work was supported in part by the Korea Institute of Energy Technology Evaluation and Planning (KETEP) and in part by the Ministry of Trade, Industry & Energy (MOTIE) of the Republic of Korea under Grant 20204010600340.

ABSTRACT Standalone rural microgrid (MG) systems are considered as a sustainable and economical solutions towards rural area electrifications. Specific control schemes are necessary to adopt for reliable and economic performance of these rural MGs. This study focuses on the optimal utilization of biomass potential considering specific applications of bio generator (BG) with BG-PV-WT-BSS and BG-PV-SMES based standalone rural MG systems. In the first case of the BG-PV-WT-BSS, the optimal sizing/selection of DGs of a rural MG has been proposed using the improved-MILP (I-MILP) approach. The objectives of this study were to minimize total net present cost (TNPC), the levelized cost of energy (LCOE) and GHG emissions. In the second case of BG-PV-SMES, the simulation model of the rural microgrid consisting of a variable speed bio generator (VSBG) and photovoltaic (PV) has been developed. Afterwards, a simplified EMS has been designed for the coordinated operation control of the distributed energy resources (DERs) in the rural MGs using MATLAB/Simulink® environment. For the DGs connected via power converter, FOSMC and FCS-MPC based coordinated control has been proposed in the simplified EMS. The purpose of the FOSMC and FCS-MPC based power converter is the improvement of the system performance (for instance power quality, regulated voltage and THD) under external disturbances. Simulation analysis shows the better operation of FOSMC and FCS-MPC under less THD and improved power quality.

INDEX TERMS Techno-economic analysis, simplified energy management system, power quality, standalone microgrid, rural electrification, hybrid energy systems, sustainable energy, social aspects.

NOMENCLATURE

BSS	Battery Storage System
COE	Cost Of Energy
DERs	Distributed Energy Resources
DGs	Distributed Generations
DR	Demand Response
DSM	Demand Side Management
EMS	Energy Management System
ESS	Energy Storage System
FCS	Finite Control Set
FLC	Fuzzy Logic Controller
FOSMC	Fractional Order Sliding Mode Control
GHG	Greenhouse Gas
HRES	Hybrid Renewable Energy System
ICE	Internal Combustion Engine
LCOE	Levelized Cost Of Energy
LPO	Load Power Observer

The associate editor coordinating the review of this manuscript and approving it for publication was Reinaldo Tonkoski.

MG	Microgrid
MILP	Mixed Integer Linear Programming
MPC	Model Predictive Control
PCC	Point of Common Coupling
PI	Proportional Integral
PR	Proportional Resonant
PV	Photovoltaic
RE	Renewable Energy
RERs	Renewable Energy Resources
SMES	Super Conducting Magnetic Energy Storage
SVPWM	Space Vector Pulse Width Modulation
THD	Total Harmonic Distortion
TNPC	Total Net Present Cost
VSBG	Variable Speed Bio Generator
WT	Wind Turbine

I. INTRODUCTION

There are many regions in remote areas of developing countries that still require electricity. Expansion of the centralized electrical power system is not feasible to these regions due to higher energy costs and power losses. Standalone electrical systems such as rural microgrids could be a possible option. It was discovered that dissimilar to bigger standalone electrical systems, rural microgrid's energy requirement is lower due to primarily domestic and street lighting loads [1]. Sustainable power with renewable energy (RE) integrations are the new pattern for energy-generating plants because of their green, and environmentally friendly energy generation [2]. Worldwide, various nations are expanding their environmentally friendly power-sharing so as to mitigate the solid reliance on fossil fuel. The most ideal choice to serve electricity to the standalone rural areas where grid-extension is impractical is by utilizing diesel or bio generator (BG). Diesel or BG have low initial investments and better voltage regulation but, generator size imposes a restriction for large power generating units. The reason is that a generator is constantly chosen depending on the value of peak load whereas more often it feeds the base-load [3]–[6]. The ongoing progress in sustainable power frameworks with renewable energy (RE) integration has resulted in their higher penetrations. Nonetheless, the primary issue with these frameworks is the climatically dependent. For such a circumstance, a hybrid energy system combining both the RE and diesel or BG is the most achievable plan.

Recently, great quanta of research attempts have been focused on standalone HRES. An optimization tool based on Sequential Linear Programming (SLP) is developed to model HRES including PV-WT and biomass fuel generators with backup units in [7]. In [8], a Genetic Algorithm (GA) based control strategy is examined to reduce the overall total net present cost and least cost of energy of a solar PV, wind, fuel cells, biogas, and biomass integrated HRES. The main aim is to determine the profitable option for electrification via the optimization process considering the hybrid energy system control, sizing, and component selection. Impact of energy dispatch strategy on the designing the size of HRES components is studied including three control strategies (simple rule-based, advanced rule-based, and dynamic programming) in [9] and results showed that feasible design options could differ depending on the control strategies. With an optimal control strategy, life cycle costs can be reduced by 5-10%. Energy management strategies consider the optimum matching of energy production with demand. To facilitate the mitigation of renewable intermittency, [10] studied a multicarrier generation scheduling scheme for standalone microgrids to dynamically optimize dispatch factors in the coupling of efficient energy conversion of an HRES containing biogas-solar-wind portfolio. The proposed optimal multi-energy scheduling scheme could accomplish higher renewable penetration and lower degradation cost while satisfying end-users' energy demand. In [11], how an MPC based EMS can perform better to improve the precision of the load forecasting algorithm for HRESs is examined. After a year of the test, the results demonstrated that 14.1% reduction in energy unbalance and 8.7% in annual operational costs were achieved when the load forecast correction was accomplished. MPC application is found in present literature including DSM-MPC in [12] for reducing fluctuations in power exchanged with the grid and preventing peaks for more favorable energy purchased from the grid.

Finite control ser model predictive control (FCS-MPC) is perceived as the most reliable methodology for online optimization of non-linear discrete state systems with multivariable control, lower current distortions, and decreased switching loss [6]. Recently, model predictive control (MPC) is attracting an increasing interest due to its simplicity, outstanding constraint handling ability, and excellent tracing principle. The two-step horizon ($N = 2$) predictive approach of FCS-MPC minimizes the switching frequency as well as a computational burden. MPC easily considers nonlinearities and constraints, calculates in advance required system signals, and the algorithm is straightforward [13]. In general, MPC is classified into two basic categories based on how the optimization is applied or performed: Finite Control Set Model Predictive Control (FCS-MPC) and Continuous Control Set Model Predictive Control (CCS-MPC) [14], [15]. CCS-MPC generates a continuous that is modulated before its application to the converter. Contrary to CCS-MPC, FCS-MPC applies the algorithm's output directly to the converter. The CCS-MPC makes use of a modulator to produce the switching signals desired for the power converter with minimum computational burden, whereas, the FCS-MPC considers the discrete nature of power converters requiring longer duration to locate the optimal option [16]. However, FCS-MPC has a drawback of the fixed time duration of voltage vector, variation in switching frequency, causing the high value of total harmonic distortion [17].

Sliding mode control (SMC) is a nonlinear variable structure controller which is applied to different power systems due to its built-in characteristic of simplicity regarding implementation, fast reference tracking, robust operation,

minimum disturbance to parametric variations and strongly applicable for VSC, electrical converters and microgrids [18]. The energy extraction from the solar PV system is implemented in [19] with a new controller design scheme for tracking the maximum power point (MPP) of a solar PV system by using a sliding mode controller (SMC) method with self-optimization.

On the other hand, fractional order sliding mode control (FOSMC) is a robust controller with a sliding surface for both additional parameters (i.e. adjustable non-integer fractional differentiator and integrator) that increase the dynamic response of the system, to ensure the convergence, providing more degree of freedom and efficient strategy to minimize the chattering phenomenon [20], [21]. In recent time, FOSMC is implemented in solving different issues of power system.

In this paper, Biomass energy potential and applications in rural areas are explored, introduced and implemented. A novel EMS with coordinated operation control is designed, implemented and verified employing a simplified simulation model implemented in MATLAB/Simulink®. The novel EMS is based on SMES control. It aims to uphold load balancing and extraction of maximum power from the PV integrated rural MG and stabilizing fixed load voltage under BG-PV generation variations. The effectiveness of FOSMC is analyzed through the MATLAB/Simulink environment. Moreover, the simulation results of the implemented FOSMC is compared with FCS-MPC and proportional-integral (PI) control.

Multiple advantages can be achieved from the proposed method for rural MGs. Some of them are, but not limited to the following:

- More efficient system due to local generating sources and electricity generation/storage.
- More reliable and secure operation because of off-grid operating capability, on-site generation control at the distribution level.
- Minimum total operating cost with the local on-site generation facilities.
- Improved rural microgrid operation by reducing production cost based on fuel and increased penetration of renewable energy resources (RERs).
- Water pumping for agricultural processing and irrigation.
- Quality power supply to a remote community in rural areas.
- Minimum fuel consumption with a reduction in greenhouse gases.
- No or less transmission losses.
- Rural street/community lighting systems for evening time activities/businesses (charging stations, internet cafes, computer/information and communication technologies (ICT) centers, local industries, rural tourism).
- Reliable supply during grid faults/interruption and demand reduction on utility grid to prevent grid failure.
- Maximum utilization of renewable energy resources (RERs) in rural areas.
- To maximize electricity access rates across rural regions.
- To promote efficient utilization of energy supply for rural communities.
- To accomplish universal access to modern energy by 2030 in reaching out to the remotest rural population.
- To highlight untapped potential points of RERs in rural areas.
- Heat generation, cooling and refrigeration/preservation for agricultural food/products and rural households.
- Availability of environment friendly green energy for rural areas.

Moreover, major portion of the population of developing countries belongs to rural areas and most of them have no access to electricity. Wind and solar PV are the cheapest sources of new energy generation in these developing communities. There is currently an over-dependence on imported fossil fuels, outdated coal technologies and hydro with expensive, seasonal and delayed generations. With the increase of renewable energy (RE) share by 2030, developing countries can have the following benefits:

- Improved energy security via diversified generation sources and reduced reliance on fossil fuels import.
- Less economic pressure through the reduction in coal and liquefied natural gas (LNG) import.
- Less energy cost will lessen the burden of additional tariff costs on prosumers and businesses while reducing the cost-tariff deficit by addressing circular debt.
- More reduced cost of renewable sources (such as solar and wind) via energy policies will support residential RE industries.
- Diversified investment in clean energy with local and international investors.
- Reduction of transmission and distribution losses. Mostly rural areas in developing countries without electricity have the following common features:
- These regions are located in remote areas with challenging terrain (for instance, hilly area, forest, desert and island). Moreover, forest areas could separate the town and placement of live electricity conductors is difficult from grids.
- These regions are situated away from electricity grids.
- These regions have deficient community members (under 500) with 2 to 200 households.
- These regions have less energy demand, probably still in the near future, due to mostly lighting load.
- These communities have the least facilities of transports and communication.
- These communities have lower income levels and less energy affordability.
- These communities have inadequate literacy level with less technical skills.

Tremendous benefits of MGs for rural electrification can be achieved. Health benefits include refrigerators for antivenom and other medicines. Social benefits include small and micro enterprise (SME) including cafe, carpentry and

tailor shops. Social benefits also include schools and vocation institutes with water pumps, study lights, and workshops on carpentry, welding and information technology (IT). Electric rice cookers will save time and high cost of cooking fuels such as wood, charcoal and kerosene. Other social benefits include extended daylight hours with solar home system (SHS) for basket weaving during night or late-night study, ironing accessibility, selling perishable food items in restaurants, operating electric rice mills, entertainment on television (TV) and electronic devices, rise of household incomes in rural community with RER based MGs, reduction of mortality rate of maternal and children due to decrease in smoke of kerosene for lighting, improved education results with high rural literacy rate due to electric lights. Economic benefits include reduction in cost compared to low qualities energy fuel and technology, light-emitting diode (LED) lighting and mobile charging facilities through MGs rather than kerosene and candles. Due to lower cost, more reliability and environmentally friendly, diesel-RER based MGs are seemly a more standard approach as compared to 100% diesel-based MGs. Moreover, MGs also provide excess electricity as back-stops during grid outage.

This paper is organized as follows: Section II talks about the methodology including the complete hybrid model including VSBG controller, fuzzy logic controller (FLC) speed controller, LPO algorithm, MPC and FOSMC. Section III finishes up the acquired simulation results while section IV sums up the conclusion of the proposed work.

II. METHODOLOGY

The following part describes the detailed modeling and analysis for each part of the proposed rural MG system, along with the employed control techniques.

A. ECONOMIC MODELING OF THE RURAL MG

The detailed modeling of the DGs are explained in [22]. For rural MG, three types of costs are investigated in optimal sizing and selection of DGs. These costs include TNPC, COE, and annualized system cost. TNPC is the present value of all capital and operation costs minus the salvage value in a project life cycle. TNPC involves net present factor β to accumulate the investment cost, replacement cost, operation & maintenance cost, fuel cost, capacity shortage cost and salvage value to time zero [23]. The levelized cost of energy (COE) is the average cost per kWh of the useful electrical energy produced by the DGs in the rural MG. The total annualized system cost (ASC) or annualized total cost (ATC) in \$/yr is the sum of system capital cost per annum, annualized maintenance cost, and annualized replacement cost for each model component which is expressed as follows [24]:

$$\mathrm{ASC} = A_{capt,cost} + A_{maint,cost} + A_{repl,cost} + A_{fuel,cost} \quad (1)$$

Similarly, TNPC and COE can be calculated as follows [25]:

$$\mathrm{NPC} = \frac{C_{\mathrm{t,ann}}}{\mathrm{CRF(i,\ N)}} \quad (2)$$

$$\mathrm{CRF} = \frac{i(\mathrm{i}+1)^N}{i(\mathrm{i}+1)^N + 1} \quad (3)$$

$$\mathrm{COE} = \frac{C_{\mathrm{t,ann}}}{E_{\mathrm{t,ann}}} \quad (4)$$

$$\mathrm{i} = \frac{\mathrm{i}-\mathrm{f}}{1+\mathrm{i}} \quad (5)$$

where, $C_{t,ann}$ represents total system annualized cost (\$/yr), and CRF (i, N) shows capital recovery factor. Whereas i, f and N represent annual interest rate (%), inflation rate (%) and a project lifetime (yr), respectively. And Et, ann is the total electrical load served (kWh/yr). So, the objectives of this problem are as follows [23]:

$$min(TNPC) = \beta \begin{bmatrix} INVT\left(i,j,P_g,W_e\right) \\ +REPL\left(i,j,P_g,W_e\right) \\ +O\&M(i,j,Pg,We,t) \\ +Fuel(i,Pg,a,b,c) \\ +ENS(Wens) + EM(i,Pg) \\ -SALV \end{bmatrix} \quad (6)$$

where β is the discount factor to calculate the TNPC; INVT, REPL, O&M, FUEL, ENS, EM and SALV are the investment, replacement, operation & maintenance, fuel, energy not served, emission and salvage costs, respectively; and are calculated as follows [23]:

$$\mathrm{INVT} = \sum_{t=1}^{N}\left(\sum_{j=1}^{T} P_{gj}x_{jt}K_{p_{jt}} + \sum_{k=1}^{T} W_{ek}y_{kt}K_{p_{jt}}\right) \quad (7)$$

$$\mathrm{REPL} = \sum_{t=1}^{N}\left(\sum_{j=1}^{T} P_{gj}x_{jt}K_{r_{jt}} + \sum_{k=1}^{T} W_{ek}y_{kt}K_{r_{jt}}\right) \quad (8)$$

$$\mathrm{O\&M} = \sum_{t=1}^{N}\left(\sum_{j=1}^{T} P_{gj}x_{jt}tK_{om_{jt}} + \sum_{k=1}^{T} W_{ek}y_{kt}K_{om_{jt}} + P_G tK_{coe_t}z\right) \quad (9)$$

$$\mathrm{Fuel} = \sum_{t=1}^{N}\left(\sum_{j=1}^{T}\left\{a\left(P_{gjs}\right)^2 x_{jt} + b\left(P_{gjs}\right)^2 x_{jt} + c\right\}\right) \quad (10)$$

$$\mathrm{ENS} = \sum_{t=1}^{N}(W_{nts}K_{coe_t}) \quad (11)$$

$$\mathrm{EM} = \sum_{t=1}^{N}\left(\sum_{j=1}^{T} P_{gjs}x_{jt}tE_{P_{gj}}K_{em_{jt}} + \sum_{k=1}^{T} W_{ek}y_{kt}K_{om_{jt}} + P_{Gt}tE_{P_G}K_{em_{jt}}\right) \quad (12)$$

where P_{gj} is the rated power of the new generating unit type j in kW, x_jt the counter for unit j in time t. W_{ek} is the rated energy of the new storage unit type k, y_{kt} is the counter for the unit k in time t. P_G is the power from/to the grid. $K_{p_{jt}}$ and $K_{r_{jt}}$ are the costs in \$/kW. While $K_{om_{jt}}$ and K_{coe_t} are costs in \$/kWh. $K_{em_{jt}}$ is the cost in \$/tons. z is a binary variable for grid connectivity. t is the time in hours. For RER based pure

green energy, the renewable fraction in the generation-mix should be maximized or in other words the non-renewable fraction (RF) should be minimized as follows [26]:

$$\min(\text{nonRF}) = \left(1 - \frac{A+B}{\sum_{t=1}^{N} P_{Lt}t}\right)$$
$$A = \sum_{j=1}^{T}\sum_{t=1}^{N} P_{gj}x_{jt}t$$
$$B = \sum_{k=1}^{T}\sum_{t=1}^{N} W_{e_{kt}}y_{kt} \quad (13)$$

where $P_{gj}x_{jt}t$ is the energy generated in kWh by generating unit type j in time t, $W_{e_{kt}}y_{kt}$ is the energy supplied in kWh by storage unit type k in time t and $P_{Lt}t$ is the energy consumed in kWh by the load in time t. The Emissions can be minimized by putting penalty on their generation sources as follows [27]:

$$min(EM) = \sum_{j=1}^{T}\sum_{t=1}^{N} E_{p_{gj}}P_{gj}x_{jt}t + \sum_{t=1}^{N} E_{P_G}P_{Gt}tz \quad (14)$$

where $E_{p_{gj}}$ and E_{P_G} are the emissions in (tons/kWh) by the unit types j and power grid in time t. These objectives are subject to the constraints of power balance, generator's operating limit, and the battery's SOC limit [23]. Power balance is an equality constraint which ensures that the sum of all generating and storage units should be equal to peak load demand. Mathematically, it can be written as follows [28]:

$$\sum_{j=1}^{T}\sum_{t=1}^{N} P_{gj}x_{jt} + \sum_{k=1}^{T}\sum_{t=1}^{N} \frac{W_{e_k}x_{kt}}{t} \geq \sum_{t=1}^{N}\left(P'_{L_t} + P_{res_t}\right) \quad (15)$$

where $P_{gj}x_{jt}t$ is the power capacity in kW for all generation units, $\frac{W_{e_k}x_{kt}}{t}$ is the power capacity in kW for all storage units, P'_{L_t} is the peak load demand at any time t and P_{res_t} is the reserve power capacity of all the generating units.

- *The generator's operating limit is an inequality constraint which ensures that generator should be operated under specified limits as follows [29]:*

$$P_{gj_{min}} \leq P_{gj} \leq P_{gj_{max}} \quad (16)$$

- *Battery's SOC limit is also an inequality constraint which ensures that battery should be charged and discharged under specified limits as follows [30]:*

$$SOC_{max} \leq SOC \leq SOC_{min} \quad (17)$$

B. PROBLEM FORMULATION WITH SYSTEM DESCRIPTION AND CONTROL TECHNIQUES

Fig. 1 shows the optimal sizing and selection strategy of rural microgrids using proposed I-MILP strategy. The proposed integrated and generic online simplified energy management system (S-EMS) approach of a standalone rural hybrid MG system is shown in Fig. 2. The system description and control techniques is explained in the following sections [31].

1) DESIGN OF VSBG SPEED CONTROLLER

The speed variation of VSBG depends on the amount of power required to generate electricity [11]. A look-up table is employed to ensure the optimal speed response during generation of the speed reference based on the required load demand as shown below [31]:

$$P_e = P_{load} + P_{SMES} - P_{PV} \quad (18)$$

where P_e shows the required load demand from VSBG, P_{load} is the demand Power, P_{PV} is the PV Power generation and P_{SMES} is the extra power generation (addition or subtraction) from VSBG for the recovery of SMES current. Based on the power-speed curve, the bio generator (VSBG) will operation at optimal speed under the coordination of the VSBG output power generation with higher speed efficiency. The value of reference speed is calculated below:

$$P_e \rightarrow [P - Speed_{LU\ Table}] \rightarrow \omega_{ref} \quad (19)$$
$$T_{demanded} = \left(\omega_{ref} - \omega_{VSBG}\right)\left(K_p + \frac{K_I}{s}\right) \quad (20)$$

where ω_{ref} is Reference speed and ω_{VSBG} shows real rotor speed. The controlled rectifiers are implemented as a power converters for the control of output current of VSBG. The VSDG mathematical model in dq coordinates is represented as follows [32]:

$$V_d = R.i_d + p.L_d\ .i_d - \omega_e.L_q.i_q \quad (21)$$
$$V_q = R.i_q + p.L_q.i_q + \omega_e.L_d.i_d + \omega_{ef} \quad (22)$$
$$T_e = \frac{2}{3}N_p.\left[\psi_f.\ i_q - \left(L_d - L_q\right)i_d.i_q\right] \quad (23)$$

where V_{dq} represents dq-axis stator voltages where as i_{dq} shows the dq-axis stator currents. While, L_{dq} represents dq-axis stator inductances, p is differential operator d/dt, R shows stator resistance, N_p represents number of poles, ψ_f shows flux and ω_r represents rotor electrical angular speed, T_e represents electrical torque [33]. For the surface mounted permanent magnet machine (SMPMM) which is used in this paper, the dq-axis inductances are equal. Hence, the torque formula is expressed as:

$$T_e = \frac{2}{3}P_n.\left[\psi_f.\ i_q\ \right] \quad (24)$$

The d-axis current is zero for attaining maximum torque per ampere, ($i_d = 0$) [34]. The flux linkage is a constant due to the permanent magnets; there is a linear relationship between the electromagnetic torque (EMT) and the q-axis current. Hence, EMT is easily controlled with the regulation of q-axis current as:

$$T_e = \frac{P_e}{\omega_r} \quad (25)$$
$$P_e = \frac{2}{3}.P_n.\omega_r\left[\psi_f\ .i_q\ \right] \quad (26)$$

therefore, ω_{ref} can be calculated from:

$$i_{qref} = \frac{3.p_e}{2.N_p.\omega_{ref}.\psi_f} \quad (27)$$

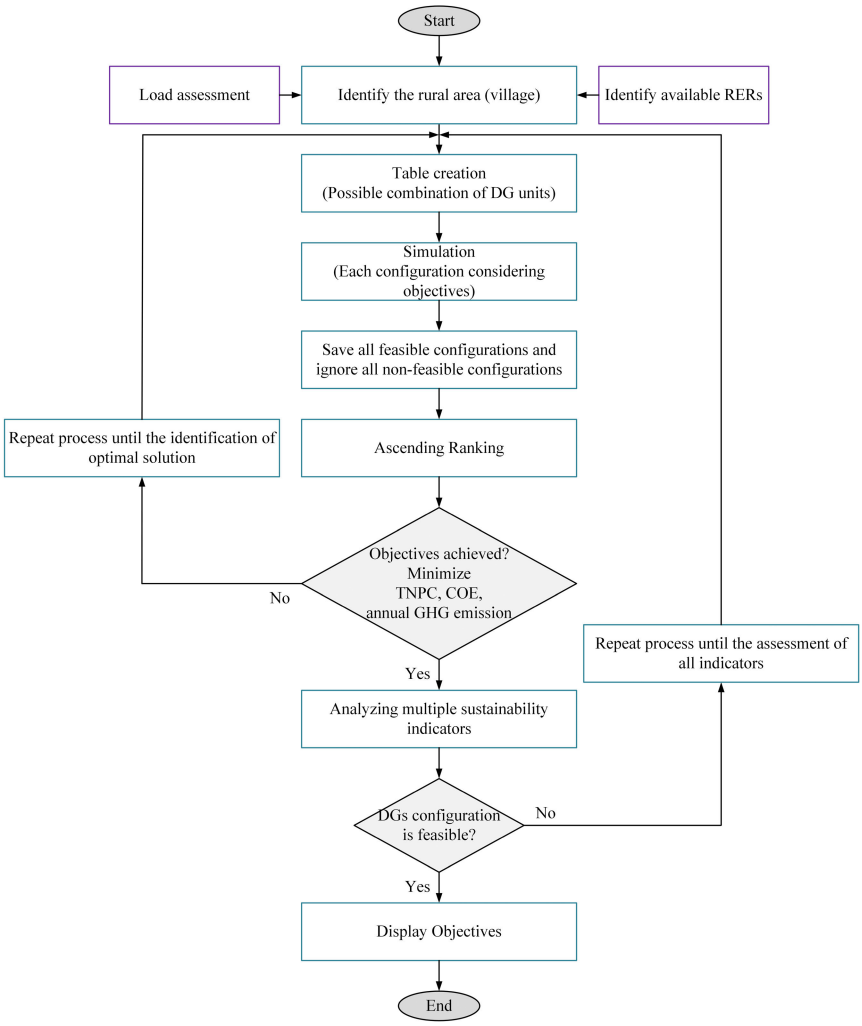

FIGURE 1. Flowchart of proposed I-MILP strategy for rural MGs.

V_{dRef} and V_{qRef} can be generated by:

$$V_{dRef} = \left(i_{dref} - i_d\right).\left(K_p + \frac{K_i}{s}\right) + \left(\omega_r.N_p.\left(L_d + L_s\right)\right).i_q \quad (28)$$

$$V_{qRef} = \left(i_{qref} - i_q\right).\left(-K_p - \frac{K_i}{s}\right) - \left(\omega_r.N_p.(L_d + L_s).i_d\right) + \left(\omega_r.N_p.\psi_f\right) \quad (29)$$

where L_s represents inductance connected in series for the compensation of generator current and limiting it to the maximum value. V_{dqRef} shows reference voltages that are implemneted for the control of power converter. Whereas the speed acceleration of VSBG is associated with the output generator power.

2) DESIGN OF SPEED CONTROLLER USING FLC

During the enhancement of generator speed by the speed controller while the power extracted from VSBG is higher, decrease in speed acceleration will occur. On the other hand, the increase in speed acceleration will occur during the low output power from the generator. When there will be a sudden shutdown of the load, the generator can undergo an over speed. To enhance the speed response of the VSBG (i.e. higher acceleration under an increased load and higher deceleration under sudden load shutdown), FLC is employed in both intervals to ensure the required value of reference current. FLC adjusts the output of the generator during accelerating mode with fast speed acceleration; while the speed of the generator will be slowed down under higher output with deceleration mode. Under steady-state operation, the value of reference current will be adjusted accordingly. The speed difference can be computed as follows:

$$Speed_{difference}(\Delta\omega) = Speed_{actual} - Speed_{reference} \quad (30)$$

The applied FLC is illustrated in Fig. 5 that has two calculated inputs (i.e., i_{qRef} and $\lambda\omega$, respectively). The input membership functions are illustrated in Fig. 3 while the output membership functions are illustrated in Fig. 5. Selector signal is employed for the control of input current to the q-current

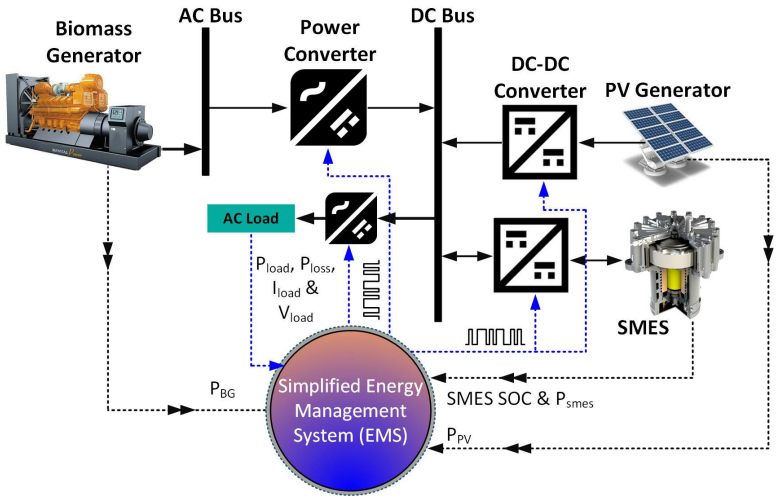

FIGURE 2. Implemented novel energy management system (EMS) of rural microgrid with configuration.

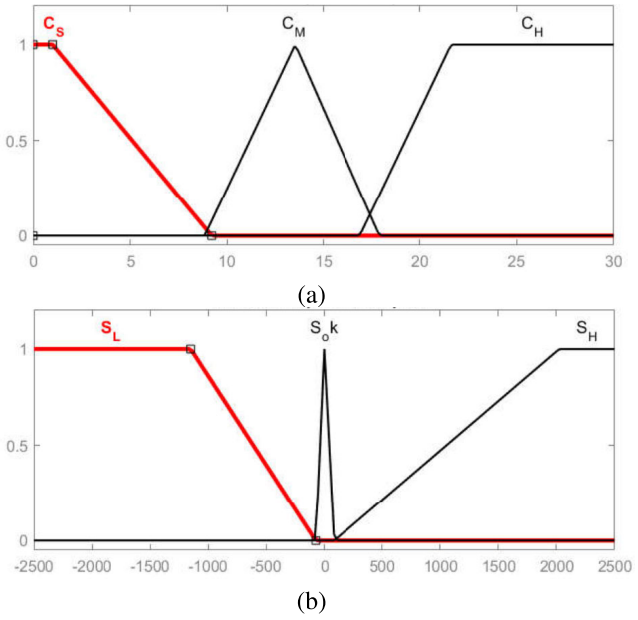

FIGURE 3. FLC Input Membership functions for a) current b) speed.

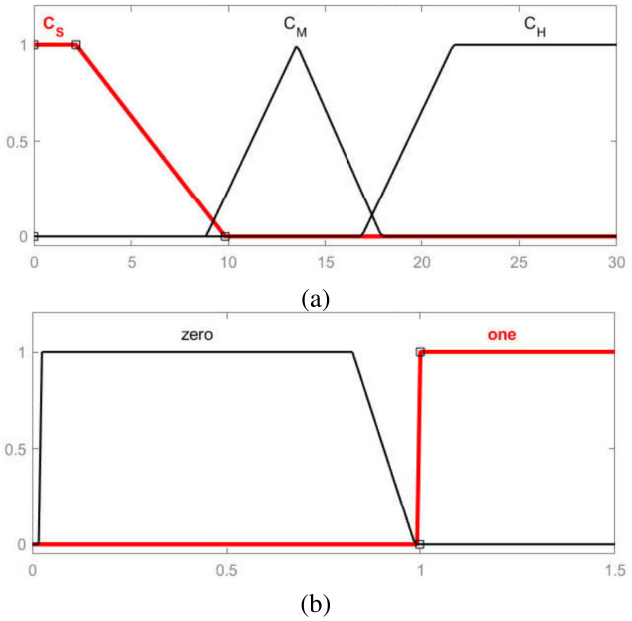

FIGURE 4. FLC output Membership map for a) Iq-current b) selector switch.

controller. Under accelerating interval, when the value of speed reference is higher compared to the real speed, the FLC will generate a small current reference to enhance the speed of a diesel engine and the switch selects reference current to q-current controller via the selector signal. Under deceleration mode, when the value of speed reference is lower than real speed, the FLC will generate a higher current reference for the speed reduction of diesel generator while the selector signal will act as a reference current to q-current controller. The implemented rules of the current reference and the selector switch are shown in Table 1 and Table 2, respectively.

From Figs. 3 & 4 and Tables 1 & 2, FLC uses membership functions for every input variable for defining the degree which effect physical values based on the variable

TABLE 1. Defined principle of current reference with selector switch.

Difference in speed ($\Delta\omega$)				
Current Reference		S_L	$S_O K$	S_H
	C_S	C_S	C_S	C_M
	C_M	C_S	C_M	C_M
	C_H	C_S	C_H	C_H

set. The FLC functional blocks such as fuzzification, rule base (inference and defuzzification. The fuzzification block performs conversion of the real number input values into fuzzy values. The fuzzy inference use the input data for the calculation of output data according to IF and THEN rules. The real numbers of output values are then converted into the defuzzification processes. In this work, the objective of

TABLE 2. Defined principle of current reference with selector switch.

Difference in speed ($\Delta\omega$)				
Current Reference		S_L	$S_O K$	S_H
	C_S	0	1	0
	C_M	0	1	0
	C_H	0	1	0

control processes is the generator speed. Generator speed is the important parameter, which decides the generator working states according to the external variations of load and PV power. Moreover, fuel utilization of the generator is always associated with the generator speed. Speed error and variable speed error are the two inputs of fuzzy controller. Speed error is compared with the reference speed and speed feedback signal which is taken from the generator output. In roder to perform the fuzzy control process, the speed error and variable speed error are taken as the input values of the fuzzy controller. The two inputs and one output of FLC are designed for this work. The input signals of FLC are speed error =(set-point speed – measured speed)/set-point speed, and variable speed error =(current speed error – previous cycle error). Moreover, the ouput values of FLC are also found as generator speed. The set of speed error, variable speed error and generator speed is CS, CM, CH, SL, SOK,SH for current (small, medium, large) and speed differene (low, zero, high), respectively. The experimental strategy is implemented to establish the rule base of FLC. The range for input and output values is [−1, 1]. Moreover, triangular membership function is selected for FLC. The fuzzy inference is the main part of FLC consisting of both experimental knowledge and decision making logics; which are then applied for deciding the selected control actions.

3) IMPLEMENTATION OF PV GENERATION WITH LPO

The output curve of the solar PV generator is non-linear, and hence it is impacted by different factors (for instance solar irradiations and temperatures). The MPPT algorithm is also variable under the meteorological circumstances. Under these conditions, an efficient strategy is needed for the extraction of maximum power at every time instant when the load is sometimes smaller than the maximum value of solar PV power generation while the storage systems are fully charged. Due to this condition, the load power observer (LPO) scheme as shown in Fig. 6 is suggested. In LPO, power is extracted from the solar PV generator based on the load demand. At each time interval, both the voltage and current of the solar PV generator are measured for the calculation of P_{pv} (t) and PLoad. The min value of P_{pv} (t), P_{Load} is compared with the value of P_{pv} (t-1) that was calculated in the previous time interval. If the output generation power is smaller than the required load power, then V_{pv} is aligned further in the same direction as in the previous time interval. If the output generation power is higher than the demanded power, V_{pv} is adjusted in the opposite direction as in the previous time interval. V_{pv} is thus regulated at each time interval of LPO. Once the demanded load power point is obtained, V_{pv} will oscillate around the optimum point that is the required point for the particular value.

4) DESIGN OF FCS-MPC

Finite control set model predictive control (FCS-MPC) with detailed modeling of FCS-MPC is explained in [24]. Mathematical equations can be represented as follows:

$$V_i - V_c = L\frac{di}{dt} \tag{31}$$

$$i - i_o = C\frac{dV}{dt} \tag{32}$$

The continuous state-space (CSS) mathematical model is:

$$\frac{dx}{dt} = Ax(t) + B_1 V_i(t) + B_2 i_o(t) \tag{33}$$

The discrete model in $\alpha\beta$-frame is:

$$\begin{aligned}\begin{bmatrix} V_{c\alpha}(k+1) \\ V_{c\beta}(k+1) \\ V_{f\alpha}(k+1) \\ V_{f\beta}(k+1) \end{bmatrix} &= \begin{bmatrix} 1 & 0 & \frac{T_s}{C} & 0 \\ 0 & 1 & 0 & \frac{T_s}{C} \\ -\frac{T_s}{L} & 0 & 1 & 0 \\ 0 & -\frac{T_s}{L} & 0 & 1 \end{bmatrix} \begin{bmatrix} V_{c\alpha}(k) \\ V_{c\beta}(k) \\ V_{f\alpha}(k) \\ V_{f\beta}(k) \end{bmatrix} \\ &+ \begin{bmatrix} 0 & 0 \\ 0 & 0 \\ \frac{T_s}{L} & 0 \\ 0 & \frac{T_s}{L} \end{bmatrix} \begin{bmatrix} V_{i\alpha}(k) \\ V_{i\beta}(k) \end{bmatrix} \\ &+ \begin{bmatrix} -\frac{T_s}{C} & 0 \\ 0 & -\frac{T_s}{C} \\ 0 & 0 \\ 0 & 0 \end{bmatrix} \begin{bmatrix} i_{o\alpha}(k) \\ i_{o\beta}(k) \end{bmatrix} \end{aligned} \tag{34}$$

The voltage vector of all switching states is represented as follows:

$$V_i = \begin{cases} \frac{2}{3} V_{dc} e^{j(i-1)} & \text{for i} = 1, 2, \ldots 6 \\ 0 & \text{for i} = 0, 7 \end{cases} \tag{35}$$

And the applied cost function is represented as follows:

$$g_v = \sum_{j=1}^{n} \left[(V_{c\alpha}^{ref} - V_{c\alpha}^{k+j})^2 + V_{c\beta}^{ref} - V_{c\beta}^{k+j})^2 \right] \tag{36}$$

5) DESIGN OF FOSMC

The comparison of FOSMC with other SMC techniques is shown in Table 3 [35]. In islanded mode, the VSC of energy storage (ES) must inject desired current at PCC depending upon the disturbance situation [36]. By applying Kirchhoff voltage law (KVL) at PCC, three-phase voltage and current equations can be written as [37]:

$$L\frac{di}{dt} = v - v_p - Ri \quad C\frac{dv}{dt} = i - i_p \tag{37}$$

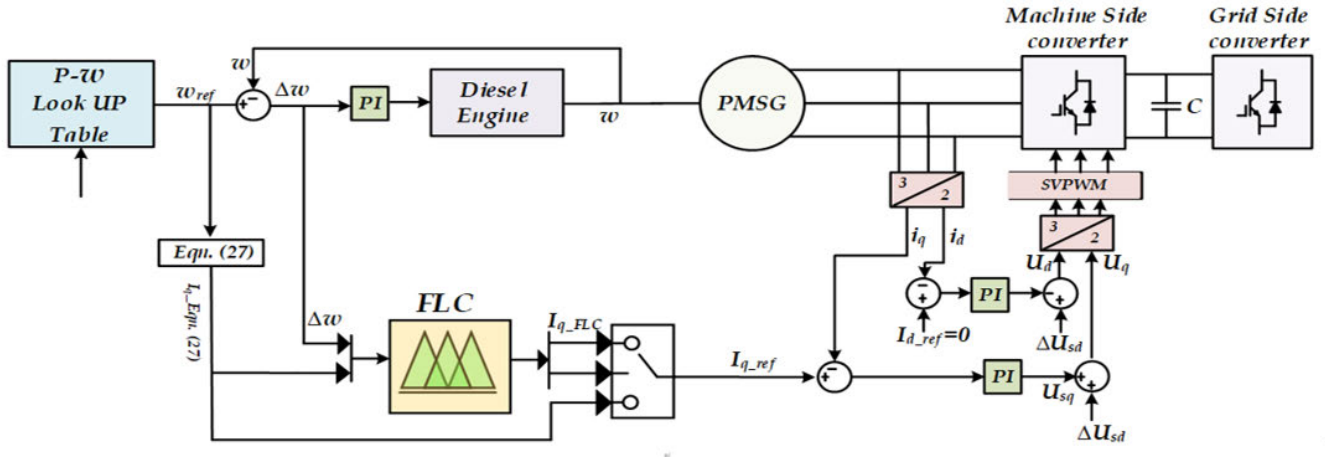

FIGURE 5. Block diagram of the suggested system.

where, v_p, i_p, v, i, R and L represent the terminal voltage at PCC, current at PCC, output voltage of VSC of ES, output current of VSC of ES and line parameters, respectively. By solving for i, we get:

$$\frac{d^2v_p}{dt^2} = -\frac{R}{L}\frac{dv_p}{dt} - \frac{v_p}{LC} - \frac{1}{C}\frac{di_p}{dt} - \frac{Ri_p}{LC} + \frac{v}{LC} \tag{38}$$

where f_d and f_q are two nonlinear functions as:

$$\begin{aligned} f_d &= 2\omega\frac{dv_d}{dt} - \frac{R}{L}\frac{dv_d}{dt} + (\omega^2 - \frac{1}{LC})v_d \\ &\quad + \frac{R\omega}{L}v_q - \frac{1}{C}\frac{di_d}{dt} + \frac{\omega}{C}i_q - \frac{R}{LC}i_d \end{aligned} \tag{39}$$

$$\begin{aligned} f_q &= -2\omega\frac{dv_q}{dt} - \frac{R}{L}\frac{dv_q}{dt} + (\omega^2 - \frac{1}{LC})v_q \\ &\quad + \frac{R\omega}{L}v_d - \frac{1}{C}\frac{di_q}{dt} + \frac{\omega}{C}i_d - \frac{R}{LC}i_q \end{aligned} \tag{40}$$

The proposed sliding surfaces for the VSC of BS under control law are defined as [37]:

$$S_d = \dot{e_d} + \lambda D^{\alpha-1}(sig(e_d)^{\gamma}) \tag{41}$$

$$S_q = \dot{e_q} + \lambda D^{\alpha-1}(sig(e_q)^{\gamma}) \tag{42}$$

where,

$$e_d = v_{dp} - v_{dref} \tag{43}$$

$$e_q = v_{qp} - v_{qref} \tag{44}$$

where, e_d and e_q represent the voltage-tracking error, $D^{\alpha-1}$ represents the fractional integral of $(\alpha-1)^t h$ order. Similarly, positive parameters α, γ and λ are design parameters (such that $\alpha < 1$ and $\gamma < 1$). The sig is defined as [38]:

$$sig(x)^{\gamma} = |x|\, sign(x) \tag{45}$$

where as, $sign$ is defined as [38]:

$$sign(x) = \begin{cases} \dfrac{x}{|x|} & \text{if } x \neq 0 \\ 0 & \text{if } x = 0 \end{cases} \tag{46}$$

TABLE 3. Comparison of SMC controllers.

Parameter	FOSMC	SOSMC	ISMC	FTSMC
Computational Complexity	Low	High	High	High
Settling time	Low	Low	Very Low	High
Control Expertise/efforts	Very High	High	Lowest	Low

The resultant relation can be written as [38]:

$$\dot{S_d} = f_d + zm_d + \tau_d + \lambda D^{\alpha}(sig(e_d)^{\gamma}) \tag{47}$$

$$\dot{S_q} = f_q + zm_q + \tau_q + \lambda D^{\alpha}(sig(e_q)^{\gamma}) \tag{48}$$

where, τ_d and τ_q are model uncertainty terms, For the VSC with a modulation index ($m = 2v/v_{dc}$) [38],

$$z = \frac{v_{dc}}{2L} \tag{49}$$

The proposed control law ensures the convergence of current tracking error on the sliding surface. The controller processes the error signals e_d and e_q, and control law generates the modulation signals m_d and m_q for the SPWM scheme for VSC of BS as [38]:

$$m_d = \frac{-\left[f_d + \lambda D^{\alpha}(sig(e_d)^{\gamma}) + K_d sgn(s_d)\right]}{z} \tag{50}$$

$$m_d = \frac{-\left[f_q + \lambda D^{\alpha}(sig(e_q)^{\gamma}) + K_q sgn(s_q)\right]}{z} \tag{51}$$

where k_d and k_d are sliding gains. Fig. 7 shows the diagram for the VSC of BS in islanded mode in dq reference frame, in which the modulating signals are found according to the suggested control laws of (50) and (51). The voltage signals in dq reference frames are used as error inputs to the FOSMC controller. Moreover sinusoidal pulse width modulation strategy is implemented for the generation of the gate signals of the voltage source inverter (VSI). The main drawback of conventional SMC is addressed here in terms of undesireable chattering phenomena due to higher switching frequency which produce higher oscillations, more

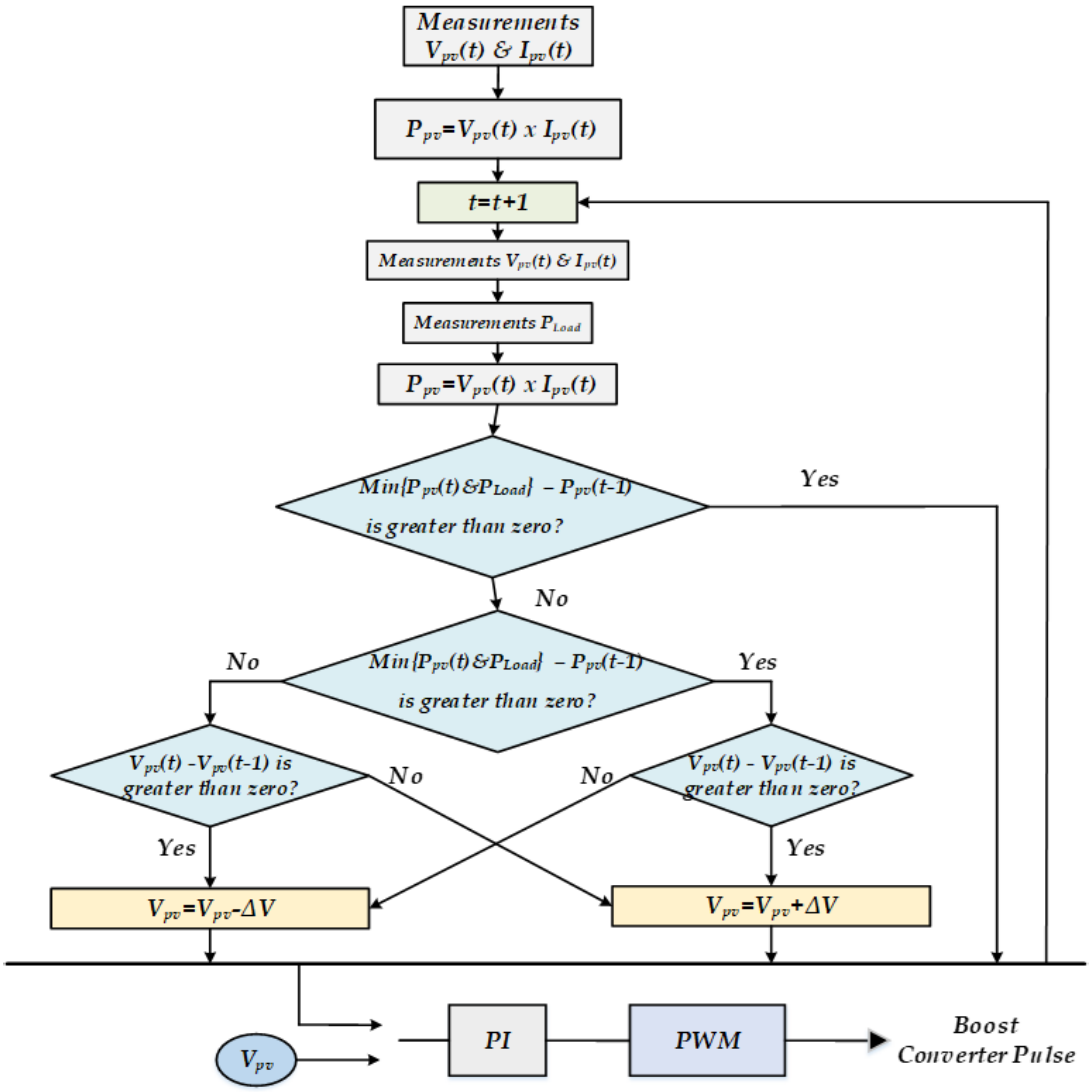

FIGURE 6. Flowchart of load power observer (LPO) Algorithm.

power losses, and lower control accuracy during the operation of the MG system. Therefore, FOSMC scheme completely reduce the chattering process and accelerates the reaching speed [39], [40].

III. SIMULATION RESULTS AND ANALYSIS

A. SIMULATION RESULTS OF I-MILP OPTIMIZATION

The residential area of Peshawar is selected with wind generation details. The estimated peak load is 6.030 kW, and the annual energy demand is 35.940 kWh per day. The load profile for two households of the selected community with detailed estimation is explained in Table 4. Fig. 8. shows wind data (speed and temperature) while Fig. 9 [41] shows solar energy data and global horizontal irradiance. Fig. 10 is the load profile.

Table 5 shows the various parameters (Input economic, PV and Wind, Biomass, battery, inverter). The detailed description of the results for the optimized model of rural MG system are described in Table 6. The battery cost is almost twice the cost of BG. The WT cost is almost half

TABLE 4. Estimation analysis of household load.

Appliance name	AC power (Watt)	Quantity	Switch ON duration (Hours/day)	Total load (Wh/day)
Lights	25	7	8	1400
Toaster	1300	1	0.1	130
Roof fan	50	3	10	1500
Microwave	1300	1	0.3	390
Air Cooler	75	1	5	375
Laptop	50	1	5	250
Blender	300	1	0.1	30
Air conditioner	1500	1	5	7500
Washing machine	500	1	0.5	250
Water Pump	500	1	1.5	750
Refrigerator	150	1	24	3600
	Total (one house)			16,175
	Total (Two houses)			32,350

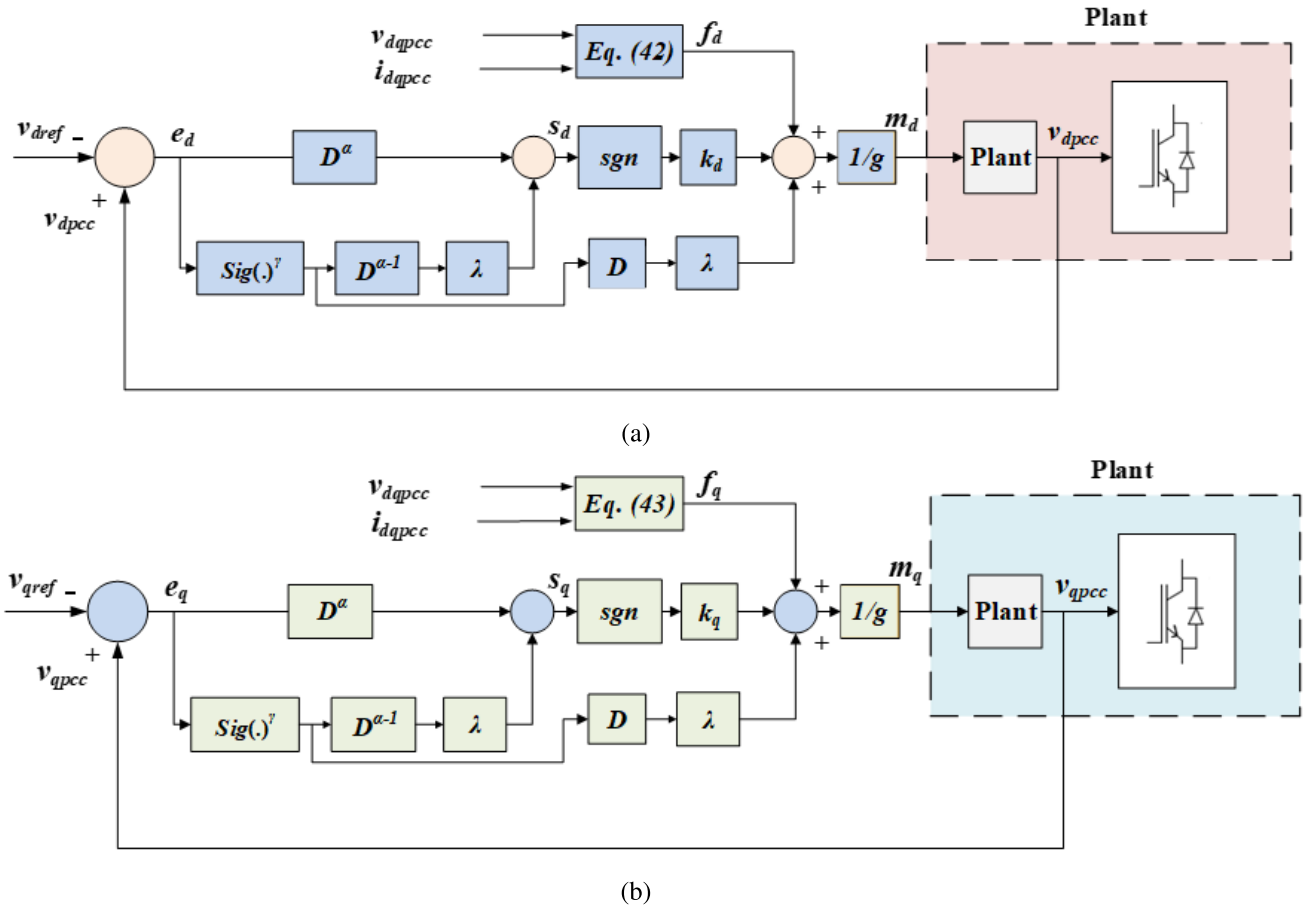

FIGURE 7. Control diagram for the VSC of BS in islanded mode (a) d reference frame, (b) q reference frame.

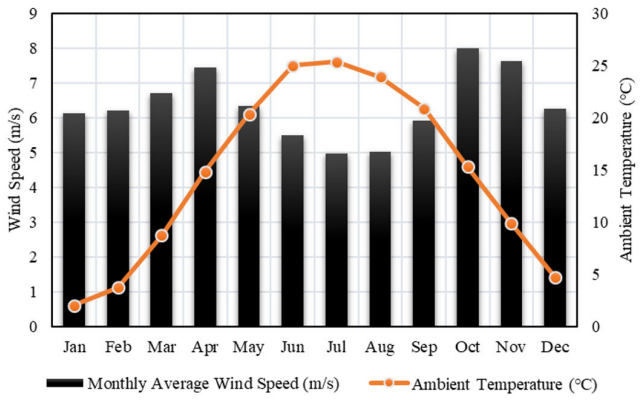

FIGURE 8. Wind profile of speed and temperature.

as compared to PV cost while PV is contributing three time to the energy demand as compared to WT. The renewable fraction (RF) is 96.9% as shown in Table 7 which shows less GHG emission for the proposed configuration plan (BG-PV-WT-ESS-Converter).

Table 8 and Table 9 shows all feasible configuration plans for the proposed site. The suggested configuration plan (BG-PV-WT-ESS-Converter) comprises of 8.99kW PV, 3kW WT, 6kW BG, 14 battery units with 5.66kW converter rating. The LCOE is 0.141 $/kWh while TNPC is $37101. The optimized system has LCOE which is 11.4 times less as compared to BG alone system (base case).

B. SIMULATION RESULTS OF CONTROL SYSTEM

The suggested scheme for rural MG design and control was implemented for the load of a proposed rural dairy industry load, where the utility grid is not available. It consists of a solar PV generating system, a VSBG as the primary power source, and a controlled super conducting magnetic energy storage (SMES) system for the regulation of power exchange between the generation and utilization. The importance of SMES based rural MG investigation is described in [42] with detailed review that only one paper out of 120 publications has considered SMES as energy storage system (ESS) in MG applications. The existence of the DC bus is helpful to incorporate multiple conventional and RE resources without requirement for AC synchronization. MATLAB/Simulink is utilized for the investigation of the suggested schemes. Parameters of both control units are shown in Table 10 whereas the mathematical model parameters with filter values are shown in Table 11.

TABLE 5. Various parameters data.

Parameter Value	Units
Input economic data	
Project lifetime	20 year
Interest rate	13.25%
Escalation rate	2%
Inflation rate	13%
PV parameters	
PV initial cost	110$ /m²
Annual O&M cost of PV	10.00$ /m²/year
Reference efficiency of the PV	25%
Efficiency of MPPT	100%
PV cell reference temperature	25°C
Temperature coefficient	0.5%
Nominal operating cell temperature	47°C
PV system lifetime	20 year
Wind parameters	
Initial cost	110$ /m²
Annual O&M cost	10$ /m²/year
Maximum power coefficient	48%
Cut-in and Cut-out speed of	2.6 & 25 m/s
Rated speed	9.5 m/s
System lifetime	20 year
Biomass parameters	
Biomass initial cost	2000$ /kW
Annual fixed O&M cost of the biogas system	$0.060/kW/year
Annual variable O&M cost of the biogas system	$0.0042/kWh/year
Biomass fuel cost of the biogas system	0.78$ / ton /year
Biomass system lifetime	20 year
Battery parameters	
Battery initial cost	85$ /kWh
Annual operation & maintenance cost of Battery	8.00$ /kWh/year
Depth of discharge (DoD)	80%
Battery efficiency	97%
Minimum & Maximum state of charge (SOC)	20 & 80%
Battery lifetime	5 year
Inverter parameters	
Inverter initial cost	250$ /m²
Annual O&M cost of inverter	0.0$ /year
Inverter efficiency	97%

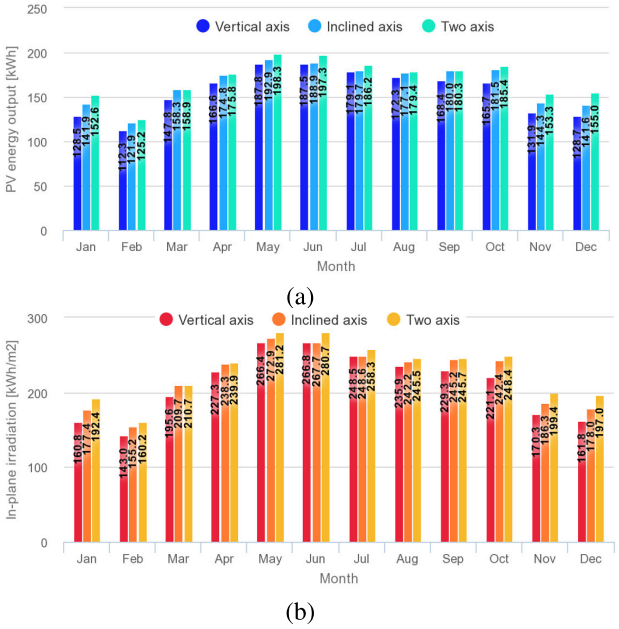

FIGURE 9. (a) Monthly energy output from PV (b) Global horizontal irradiance.

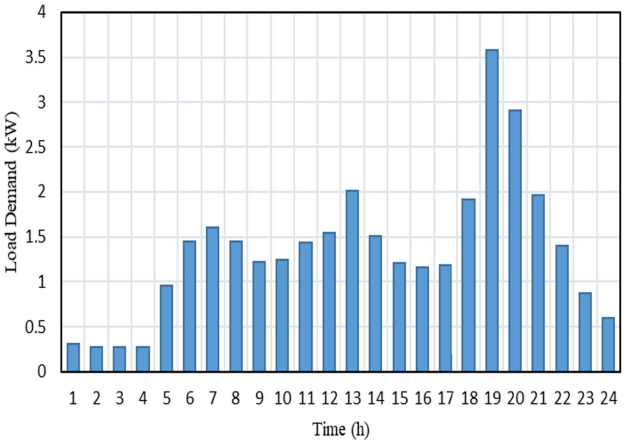

FIGURE 10. Load curve of two households.

1) CASE-I: SVPWM-PI

The PI control with FLC is implemented and Fig. 11 represents the speed response of the PI control that obviously shows that the real speed is following the reference speed. Speed controller with FLC provides a better performance while the speed tracks the required speed much faster under accelerating mode and the speed of VSBG also reduces much faster under the de-accelerating mode. Fig. 12 illustrates the output generation and load powers of DERs (PV and VSBG) with fixed unbalanced load by utilizing PV MPPT with FLC. The load power observer (LPO) is implemented for the prevention of PV from excess generation of power which will be more than load requirement. The solar PV power is same as the load demanded power plus the power needed for charging the SMES unit and this scheme will save SMES from overcharging. At time t = 1 sec, the PV power and Pvsdg both are low, still it is supplying load power to 1 PU. The difficient power is suppied by energy storage system i.e. SMES in this case. The SMES current is shown in Fig. 13. Fig. 14 illustrates the dc voltage that represents a stable performance with a better SMES response. Fig. 15 illustrates q-current response using FLC. Fig. 16 illustrates the difference in speed between reference and real value of the speed that is almost equal to zero during the simulation interval. Fig. 17 illustrates load voltage with the zoomed value is represented in Fig. 18. And load current with zoomed graph are shown in Fig. 19 and Fig. 20, respectively. It is evidently noticed that the waveform is not a pure sinusoidal due to the different values of positive and negative peaks. Output power is also ilustrated in Fig. 21.

2) CASE-II: FCS-MPC

The system performance is exceedingly enhanced under the implementation of the suggested FCS-MPC scheme. Fig. 22 illustrates load voltage that is ripple-free. The load current is shown in Fig. 23.

TABLE 6. Detailed description of the optimized MG model.

Comp \ Cost($)	Initial	Replacement	O&M	Fuel	Salvage	Total
BSS	$2,450.00	$8,758.60	$2,493.24	$0.00	$0.00	$13,701.85
PV	$7,189.83	$0.00	$2,000.67	$0.00	$0.00	$9,190.50
WT	$2,700.00	$2,251.13	$667.83	$0.00	($1,613.32)	$4,005.64
Bio Generator	$12,000.00	$0.00	$729.27	$2,128.64	($7,385.43)	$7,472.49
System Converter	$1,699.21	$1,482.60	$0.00	$0.00	($451.26)	$2,730.56
System	$26,039.04	$12,492.34	$5,891.02	$2,128.64	($9,450.01)	$37,101.03

TABLE 7. Electricity generation/utilization in kWh/yr of the optimized MG configuration.

Production	kWh/yr	%	Consumption	kWh/yr	%
PV	13,471	73.0	AC Primary Load	11,808	100
Bio Generator	370	2.00	Excess Electricity	5,478	29.7
WT	4,621	25.0	Unmet Load	0.0	0.0
Total	18,462	100	Capacity Shortage	0.0	0.0
-	-	-	Renewable Fraction (RF)	-	96.9

TABLE 8. Feasible configuration plans based on NPC.

Case	HRES Plan	TNPC ($)	LCOE ($/kWh)	RF (%)	DG Opr. (hr/yr)	GHG (kg/yr)
1	BG-PV-WT-ESS-Converter	37101	0.141	96.9	91	321
2	PV-WT-ESS-Converter	37885	0.144	100	0	0
3	BG-PV-ESS-Converter	42952	0.163	94.5	146	552
4	PV-ESS-Converter	47946	0.183	100	0	0
5	BG-WT-ESS-Converter	70991	0.270	89.7	239	1005
6	BG-ESS-Converter	183471	0.698	0	2377	11047
7	BG (base case)	422510	1.610	0	8,760	17488

TABLE 9. Feasible configuration plans based on optimal design.

Case	Component sizing					Cost results				
	PV(kW)	WT(Qty)	BG(kW)	ESS(Qty)	Converter(kW)	Initial($)	Replacement($)	O&M($/yr)	Bio Fuel($)	Salvage($)
1	8.99	3.0	6.0	14	5.66	$26,039.04	$12,492.34	$5,891.02	$2,128.64	($9,450.01)
2	13.3	3.0	-	18	5.56	$18,143.05	$14,968.39	$6,829.73	$0.00	($2,056.54)
3	11.4	-	6.0	18	6.00	$26,089.16	$12,831.60	$6,918.74	$3,661.03	($6,548.89)
4	15.5	-	-	30	5.59	$19,358.11	$20,231.46	$8,801.86	$0.00	($445.30)
5	-	21	6.0	24	5.66	$36,798.67	$32,254.79	$10,864.31	$6,665.32	($15,592.44)
6	-	-	6.0	24	5.45	$17,836.17	$70,016.68	$23,323.41	$73,279.25	($984.24)
7	-	-	6.0	-	-	$12,000.00	$225,258.08	$70,202.63	$116,005.45	($956.04)

TABLE 10. Details of control parameters.

Controller	Parameter	K_p	K_i
Rectifier control	Outer loop gains	5.0	25.0
	Inner loop gains	1.06040	0.89130

TABLE 11. Details of model parameters.

Filters	Parameter name	Values
Machine side filter, L_CM=2.50mH,	SMES inductance(L_S)	6H
C_MS=50μF	Resistance(R_A)	17Ω
Output filter, R=0.10Ω, L=6.0mH,	Resistance(R_B)	24Ω
C=250.0μF	Resistance(R_C)	24Ω

3) CASE-III: FOSMC

The improved performance of the proposed rural MG model is observed after applying the suggested FOSMC scheme. Fig. 24 shows three-phase output voltage. The three-phase load current is shown in Fig. 25.

4) CASE-IV: TOTAL HARMONIC DISTORTION (THD)

Ripples are reduced significantly with FCS-MPC and FOSMC as compared to PI controller. Fig. 26 illustrates the THD under PI control that is higher in value (i.e. 4.92%) as compared to the FCS-MPC and FOSMC controllers which are only 2.03% and 2.21%, respectively. Hence, the better performances of FCS-MPC and FOSMC controllers are observed.

5) CASE-V: EXPERIMENTAL RESULTS OF FOSMC AND PI

It is obvious from Fig. 29 that the settling times of the speed responses are 0.18 s and 0.09 under the PI and FOSMC control at startup transient time. it also can be seen that the speed drop under the control of PI, and FOSMC methods is 700 and 400 rpm, individually. Moreover, the current responses under the PI and FOSMC methods at a reference speed of 1500 rpm with motoring load of 10 Nm is added at 5 s, which are

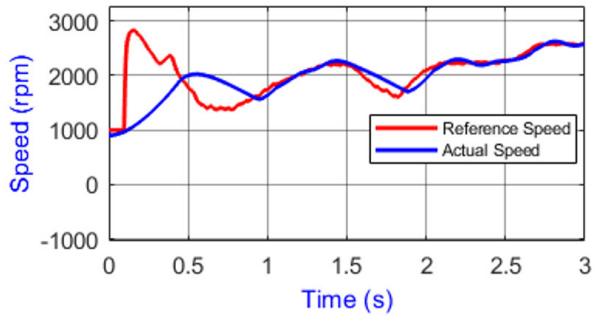

FIGURE 11. Speed response between reference and actual value of VSBG using FLC.

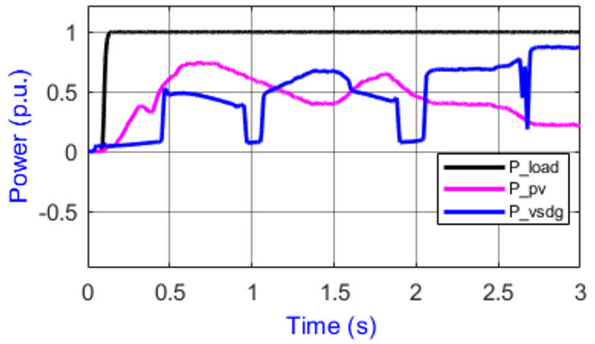

FIGURE 12. Output load power under a fixed load.

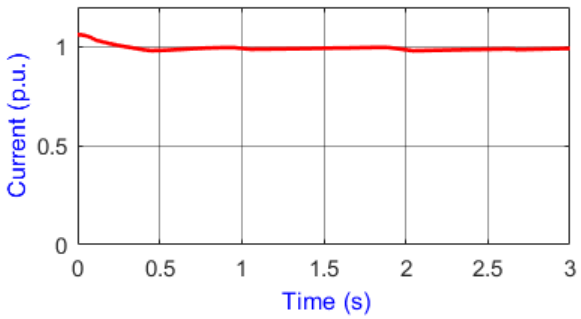

FIGURE 13. The SMES current.

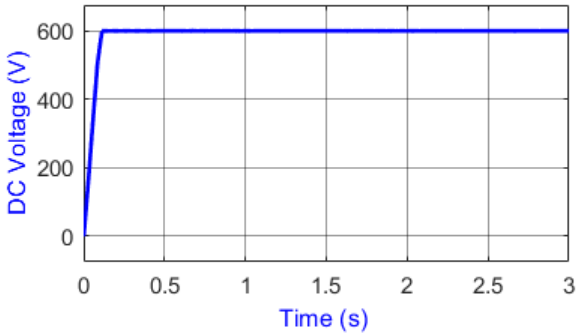

FIGURE 14. DC voltage waveform at the input side of load inverter.

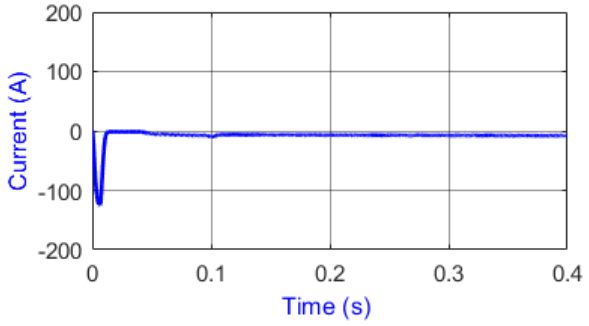

FIGURE 15. Q-Current waveform.

shown in Fig. 30. As seen from this picture, the FPSMC method has fastest transient response, smallest current ripple and chattering than PI method, respectively. Therefore, it can be concluded that FOSMC is much faster under transient time, smooth in steady state operation and smaller current ripple under whole operation than that of PI, respectively. The oscilloscope results for speed responses under the PI and FOSMC controls are shown in Fig. 31 and Fig. 32, respectively. Figures 31 and 32 are the experimental results and the per division units of x-axis and y-axis are expressed in terms of time (s) and current (A), respectively. Moreover, the Figure 31 and 32 are the experimental results, which are taken from the oscilloscope as picture (PNG). Therefore, the legends are already mentioned in the Figure 31 and 32 for the speed, current and time as rpm, ampere (A) and second (s), respectively under the load and no-load conditions. Moreover, the data of the speed, current of experiments are plotted in the Matlab for better comparison of the PI and FOSMC, under the load and no-load, which are shown in Figure 29 and 30, separately.

C. CRITICAL ANALYSIS AND DISCUSSION

First, optimal sizing of PV integrated rural MG system is proposed for the specified rural area. Second, coordinated control integrated into simplified energy management system (EMS) is proposed for the feasible rural MG system. Moreover, three control techniqes such as proportional integral (PI), finite control set model predictive control (FCS-MPC) and fractional order sliding mode control (FOSMC) are implemented for the voltage control of load side converter. FLC is generating speed reference. These controllers are related to the control of voltage source converter and therefore they are tracking the output of VSC up to the desired reference. Third, experimental verification of PI and FOSMC are investigated for practical motor load such as water pumping system for irrigation purpose. The noteworthy results of the proposed PV-WT-BG-BSS converter based rural microgrid system are closed beneath:

- *The optimal hybrid rural MG is the BG-PV-WT-BSS-Converter system, which contains an 8.99 kW PV, 3 kW WT, 6 kW BG, 5.66 kW power converter and 14 battery*

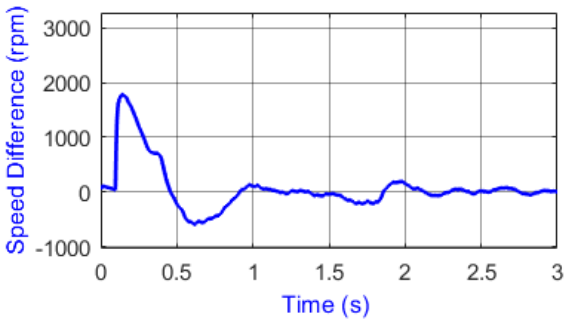

FIGURE 16. Difference in speed between reference and real value of VSBG.

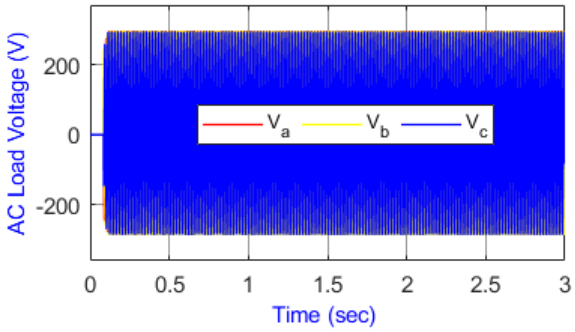

FIGURE 17. Load voltage during PI control.

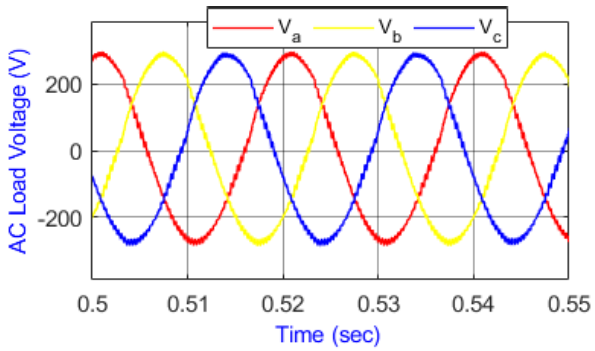

FIGURE 18. Zoomed load voltage during PI control.

storage system with 2.37 kWh each. This configuration corresponds to an investment cost of $26,039, an operation cost of $5,891/yr, a TNPC of $ 37101 and a levelized COE (LCOE) of $0.141/kWh under load following (LF) dispatch strategy.

- *Negligible GHG discharge is found and less bio fuel utilization is not required for the proposed rural MG model. While 321 kg/yr emissions are found.*
- *The reduction of capital and replacement cost of bio generator has a significant impact on the optimal configurations, TNPC and levelized COE. The BG-PV-WT-BSS-Converter is found to be the most optimal configuration for the selected rural area. While PV-WT-BSS-Converter (pure green energy) is the second most optimal configuration. It is found that a PV-based BG-BSS-Converter system is more feasible with about half TNPC and COE as compared to WT-based Diesel-BSS-Converter system. As compared to the cost of the BG-based system (base case), the ratio of the TNPC for the BG-PV-WT-BSS, PV-WT-BSS, BG-PV-BSS and BG-WT-BSS systems are 10.4%, 10.2%, 8.8% and 7.8%, respectively. The TNPC and COE values of the BG-WT-BSS system increase twice as compared to PV-WT-BG-BSS and Diesel-PV-BSS systems, while almost six times reduction as compared to BG-only system.*

TABLE 12. Details of controller parameters.

Reference	Control strategy	% THD	Control Complexity
[43]	PI	16.0	Low
[44]	Dead Beat	2.10	Medium
[45]	PR	1.40	Low
[46]	Adaptive Control	0.53	Low
[47]	Implicit-MPC	2.93	Medium
Present Study	PI	4.92	Low
	FOSMC	2.21	Low
	FCS-MPC	2.03	Low

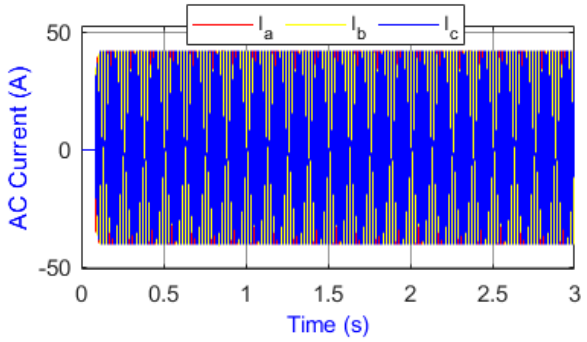

FIGURE 19. Load current under PI control.

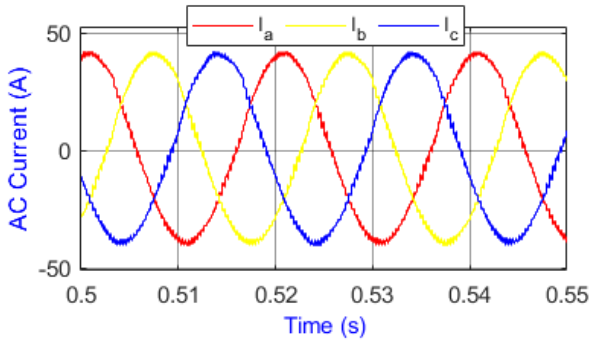

FIGURE 20. Zoomed load current during PI control.

The noteworthy results of the proposed BG-PV-SMES based rural microgrid system are closed beneath:

- *A novel EMS with coordinated operation control is designed and verified employing a simulation model developed in MATLAB/Simulink® software.*

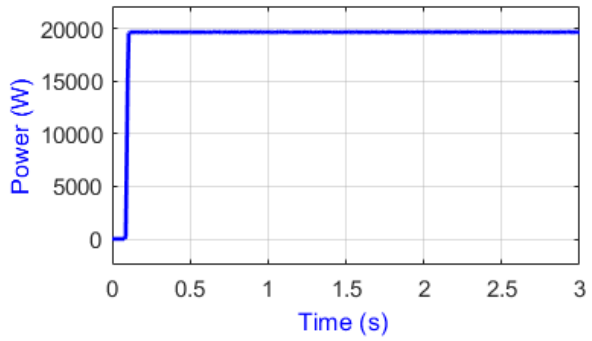

FIGURE 21. Three-phase load power during PI control.

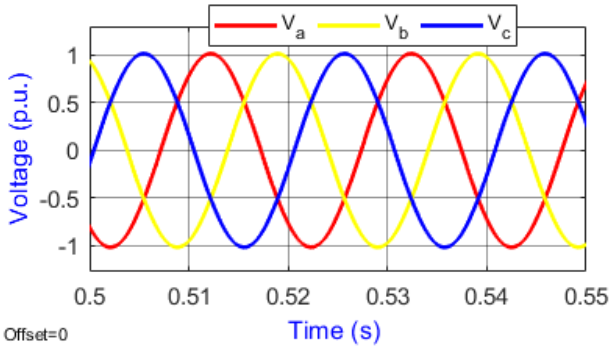

FIGURE 22. Zoomed load voltage under FCS-MPC control.

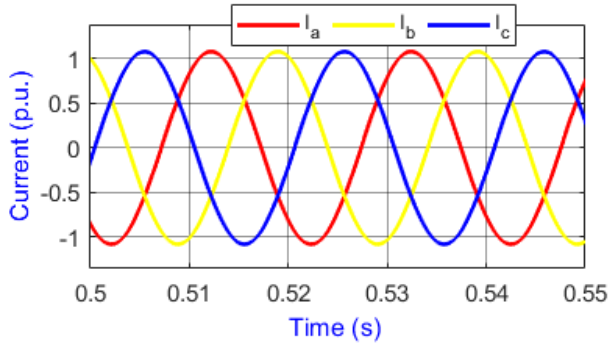

FIGURE 23. Zoomed load current under FCS-MPC control.

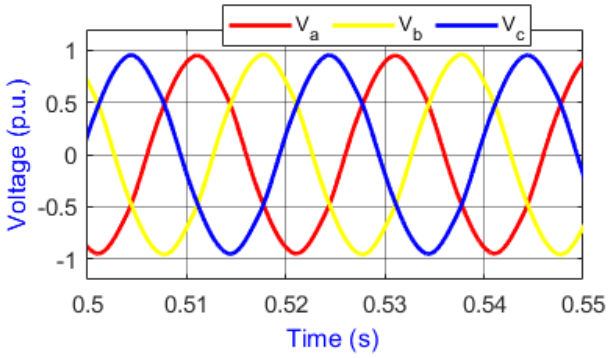

FIGURE 24. Zoomed load voltage under FOSMC control.

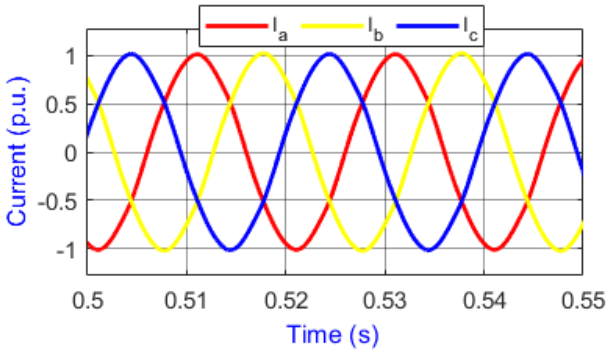

FIGURE 25. Zoomed load current under FOSMC control.

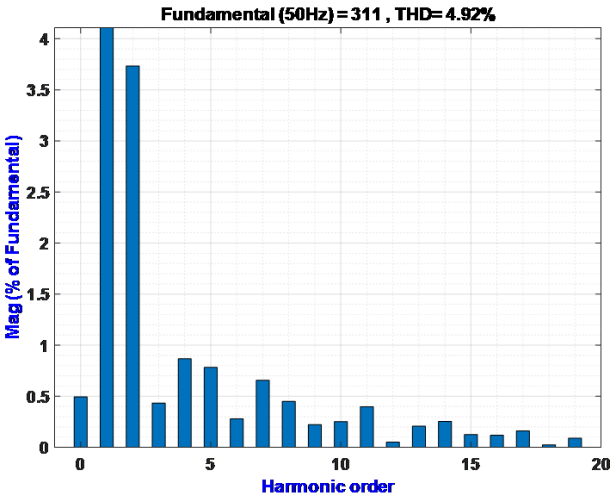

FIGURE 26. Voltage THD spectrum with SVPWM-PI.

The simplified EMS with load power observer (LPO) is based on SMES. It aims to maintain load balance and extract maximum power from the optimal rural MG and regulating AC bus voltage during PV and BG generation fluctuations and abrupt load changes.

- *FOSMC and FCS-MPC are implemented and built for optimal operation of the rural MG. As compared to traditional linear PI control with complicated feedback loops, slow dynamics and time-consuming PI tuning, the FOSMC and FCS-MPC can balance power in a fast and safe manner when load changes.*
- *During unbalanced loads, the PCC voltage is regulated much faster with great accuracy after each switching interval. Comparison of results with the PI-based controller shows much better performance under transient and steady-state conditions for the proposed schemes. The brief voltage dip due to switching of a heavy load can be controlled rapidly by the suggested schemes under better settling time compared to the PI-based controller strategy.*
- *The control schemes enable a faster and accurate voltage control during connection of the BG to a host standalone rural MG. The proposed control schemes present*

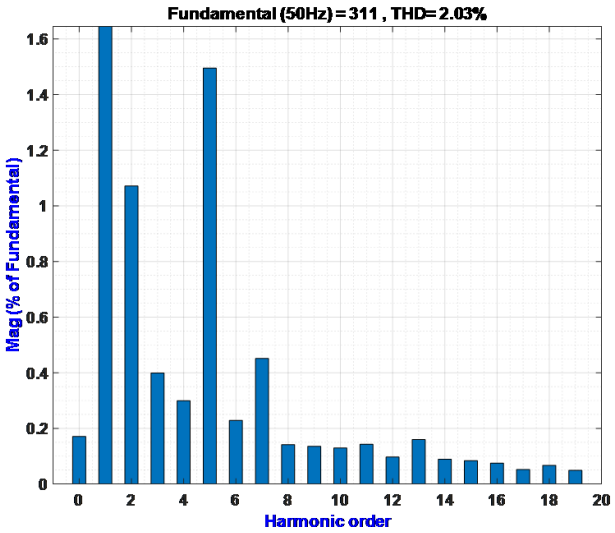

FIGURE 27. Voltage THD spectrum with FCS-MPC.

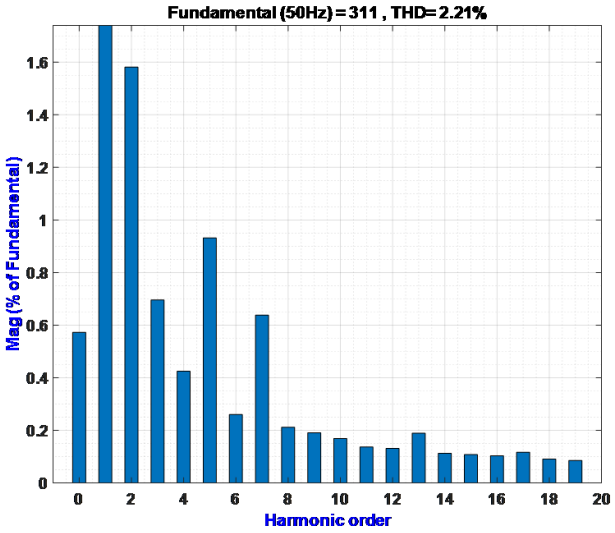

FIGURE 28. Voltage THD spectrum with FOSMC.

much better performance under transient and steady-state conditions compared to the PI-based controller.

- *For robustness assessment, stable performance of the suggested schemes and accurate control of the PCC voltage are observed during the external disturbances of RERs and load.*
- *In this control scheme, a single step prediction horizon is applied for FCS-MPC. Hence, it has a light burden of computations. This feature is very crucial for online control cases and practical implementation.*

For optimal sizing, MILP scheme is applied by considering real load demand curve of specified rural area. For coordinated control integrated into EMS, only one case study with constant load is simulated and analyzed in this paper in order to avoid complexity and pages length of the paper. However, the future extension of this work also includes incorporation of real load demand curve including different types of loads such as linear, unbalanced and non-linear loads for different applications of rural areas electrification.

D. EXPLANATIONS WITH THEORETICAL BACKGROUND

There are various factors which should be considered by the engineers and planners during the designing phase of the rural microgrid systems, which includes. Following are overall considerations for designing rural MGs:

- The power network is only accessible to limited prosumers due to a specific layout.
- There is a variety of loads ranging from single-phase to medium capacity three-phase. For instance, irrigation water pumping requires three-phase power supplies.
- The system reliability requirement is under average. The following questions need to be answered for the estimation of loads and PV generations:
- What will be the structure of the rural microgrid system in order to meet the loads?

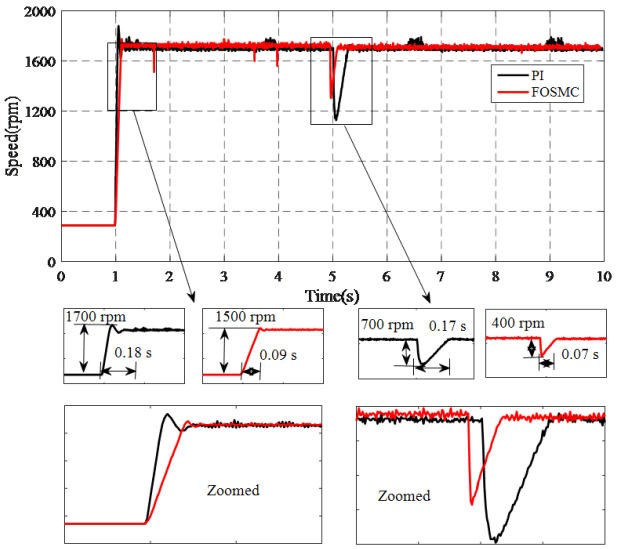

FIGURE 29. Speed responses under the PI and FOSMC control.

- What will be the sizing criteria of rural microgrid components?
- Where will the PV based DERs be installed? Following are the inputs which are required during the design procedure:
- The available local resources of power generation with their precise locations.
- The possible restrictions in terms of roads and different kinds of obstacles.
- The possible future growth in community loads, business opportunities and living standards.
- The estimated costs of PV based DERs with other accessories, the significant costs including installation and operation.

The design objectives include optimal sizing of rural microgrid with the following constraints:

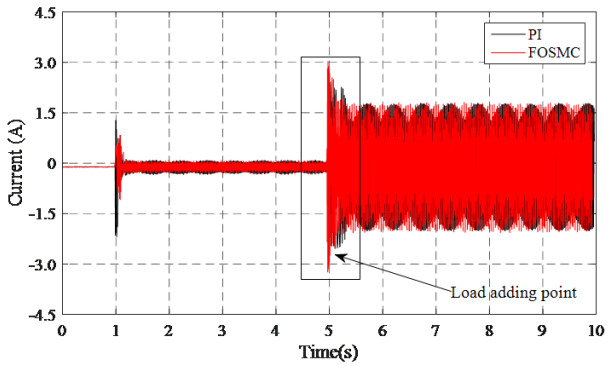

FIGURE 30. Current responses under the PI and FOSMC methods at a reference speed of 1500 rpm with motoring load.

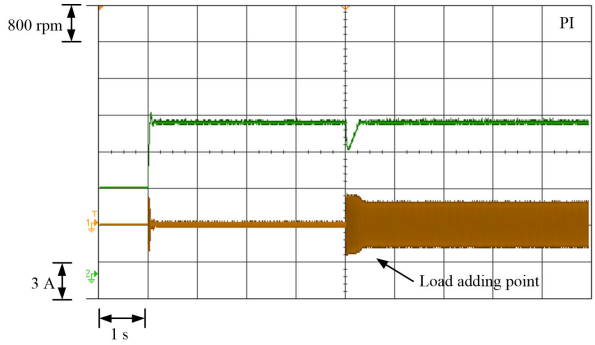

FIGURE 31. Oscilloscope results for speed responses under the PI control.

- From the perspective of energy balance, analyzing the minimum possible sizes of PV based DERs for continuous and reliable electricity supply to the targeted community loads.
- Considering the practical component parameters for the design of PV based DERs.
- Justifying the need of deployment of available RERs in rural areas.
- Designing a feasible PV based standalone rural MG systems.
- Assessing the suggested MG performance by employing the real village load, authentic sources data and realistic prices of MG components.
- Analyzing the impact and feasibility of bio generator use to reduce GHG emissions.
- Analyzing the influence of sustainability indicators on levelized cost of energy (LCOE) and total net present cost (TNPC) of the MG system.

Further explanation of the proposed rural microgrid systems are closed beneath:

- MGs based on RERs need energy storage systems to handle the power unbalancing, which is particularly caused due to variable and intermittent behavior of RERs. However, higher costs and limited life span depending on charging and discharging cycles limit energy storage applications. The life of energy storage bank can be improved with the help of optimized operation control by controlling the charging and discharging. Inevitably, the optimized operation control of energy storage bank in a MG based on RERs need to be coordinated with the control for achieving other control objectives. For example, how to improve the efficiency of the MG under different system conditions will be naturally involved in the designing of control scheme of the MG. Therefore, the optimal control of MG based on RERs certainly is multiple objectives ones.

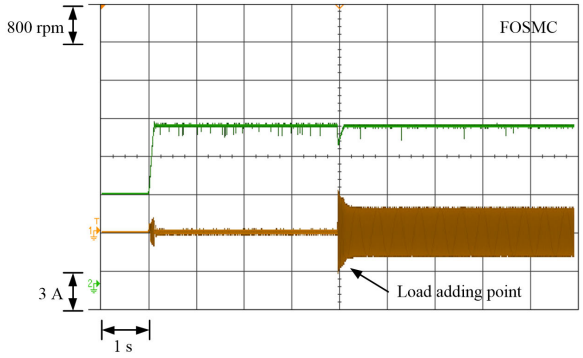

FIGURE 32. Oscilloscope results for speed responses under the FOSMC.

- One of the major goals of the future intelligent or smart microgrids is to shift towards 100% electricity production from RERs. However, the disparate, intermittent, and typically widely geographically distributed nature of RERs complicates the integration of RERs into the MG. Actually, the curtailed RER generation systems due to their intermittency is the biggest problem delaying the transition towards pure green renewable energy integration into the MG system. But, despite all this, a pure green rural MG system with suitable capacity ESS can be controlled to operate well by developing the robust control system for stabilizing the fluctuating and intermittent RERs.
- In low voltage distribution networks, voltage unbalance is viewed as one of the fundamental power quality issues in three phase microgrid systems. It has a critical effect at the distribution level to voltage sensitive loads. Uneven distribution of single-phase loads is one of the significant reason causing a voltage to unbalance. Traditionally, an active filter can be applied with the distribution lines for lessening the degree of voltage unbalances. Another possible way is to infuse negative sequence current to adjust the flow in the distribution lines and compensate unbalancing. Nonetheless, all these techniques require extra compensation hardware, which may increase the total investment cost of rural MG. In the MGs framework, the high usage of interfacing converters makes it conceivable economically to utilize DG units to improve the voltage unbalance of rural MG.
- Power quality is an important aspect for the reliable and economic operation of MGs. And total harmonic

distortion (THD) is a widely accepted standard index for the assessment of power quality. Currently, MGs are generally designed with higher penetration of RERs, which are connected through power converters. The operation of switching converters and nonlinear loads alter the power characteristics of distribution networks by introducing unwanted harmonics to load current and bus voltage. Also, for the MGs connected to main grids, the unwanted harmonics from them may cause a severe power quality degradation on point of common coupling (PCC). To tackle the harmonic problem of MG, effective control methods are essential, which are required to reduce the total THD to less than 5% (according to the IEEE 519 standard) because traditional methods to control harmonics are very expensive and not adequate for rural MGs. Compared to the existing conventional schemes, the least possible THD of MGs may be achieved without expensive cost by employing optimal control strategies in converters. For instance, FCS-MPC and FOSMC are offering advantages of multi-variable control with fast and robust dynamic response, if is used in the converters of rural MGs, multiple rigorous requirements of voltage balance and low harmonics may be simultaneously handled. Besides, FCS-MPC is more intuitive in implementation as compared to classical control methods.

- It is advisable to design a kind of integrated EMS with low cost for automatically optimizing operation of rural MGs. Due to rising cyber-attacks and cyber-mistakes, the major issue is to choose a particular area with proper architecture and guidelines for implementing a robust and stable integrated EMS of rural MG operation. On other hand, the integration of RER based DGs in the main grid or in grid-forming islanded MG is increasing as the most alternative promising solutions to large traditional centralized power stations for the rural area electrification. So, the stability control of MGs is becoming more complicated due to the high penetration of RER and the switching of MG operation modes.
- To sum up the above, the integrated EMS of rural MGs should be a multi-function ones that integrates coordinated control of DGs and loads for system stability, device protection, load scheduling, energy management (ESS efficiency and lifespan, utilization of renewable resources etc.) and improvement of power quality.
- The proposed integrated EMS with coordinated control method, which simplifies the control structure and facilitates the parameter design. In the proposed integrated EMS, the full state-variable FCS-MPC is used to manipulate the power switches directly in order to attain rapid tracking of the reference signals. The architecture of the proposed scheme is suitable to achieve the superior performance of multiple control objectives, the capacity of easy upgradation and expansion of DGs in plug-and-play mode, the robustness of operation and the resiliency to communication failure.
- An integrated EMS with coordinated operation control is designed and verified employing a simulation model developed in MATLAB/Simulink® software. The developed EMS is based on generator speed control with charging/discharging of ESS. It aims to maintain load balance and extract maximum power from the optimal rural MG and regulating AC bus voltage during PV power fluctuations and abrupt load changes, meanwhile keeping the ESS charging within the allowable limits.
- FCS-MPC and FOSMC are implemented and built for optimal operation of the rural MG.
- As compared to traditional linear control with complicated feedback loops, slow dynamics and time-consuming PI tuning, the FCS-MPC and FOSMC based interlinking power converter (IPC) can balance power in a fast and safe manner when load changes.
- During unbalanced loads, the PCC voltage is regulated much faster with better accuracy after each switching interval. Comparison of results with the PI-based controller shows much better performance under transient and steady-state conditions for the proposed FCS-MPC and FOSMC based schemes. The brief voltage dip due to switching of a heavy load can be controlled rapidly by the suggested EMS scheme under better settling time compared to the PI-based controller strategy.
- The regulation performance of the controller is proper and fast when switching loads. The control scheme enables a faster and accurate voltage control during connection of the load to a host standalone rural MG. The proposed control schemes present much better performance under transient and steady-state conditions compared to the PI-based controller strategy.
- For robustness assessment, mismatch for RLC filter values show stable performance of the suggested scheme and accurate control of the PCC voltage are observed during the external disturbances of RERs and load.
- In this MPC control scheme, a single step prediction horizon is applied. Hence, it has a light burden of computations. This feature is very crucial for online control cases and practical implementation.

IV. CONCLUSION

First, this study accomplished an optimal system of PV/WT/BG/battery based rural MG under the intermittent RERs. The techno-economic analysis is implemented with the proposed I-MILP scheme. Feasible sizes of rural MG are obtained with the most viable option under PV, WT, battery and converter units. Practical load with meteorological data is used for the investigation of simulation results. The feasible option with PV/WT/BG/battery units is achieved with the minimum TNPC of $37101 and LCOE of 0.141 $/kWh. Hence, 96.9% RERs is ensured with no electricity shortage. The vital function of BG with emission is discovered for islanded rural MG. Therefore, BG-only is not encouraged during islanded mode. The carbon emission of the proposed system is only 321 kg/yr. The proposed model comprises

TABLE 13. Literature studies for the optimal design and operation of rural microgrids.

Ref-Year	System Component Details	Offline EMS	Online EMS	Practical Data (Load/DERs)	Experimental Analysis	Region
[48]-2020	PV	Yes	No	Load	No	Tanzania
[49]-2020	PV-BSS	Yes	No	Both	No	China
[50]-2020	PV-BSS	Yes	No	Load	No	-
[51]-2019	BSS-Grid	Yes	No	Load	No	China
[52]-2018	Diesel-PV-WT-BSS	Yes	No	Both	No	Rwanda East Africa
[53]-2018	Diesel-PV-BSS	Yes	No	Load	No	-
[54]-2017	Diesel-PV-WT-BSS	Yes	No	Both	No	India
[55]-2017	Diesel-PV-WT-BSS	Yes	No	Both	No	Eastern Cape South Africa
[56]-2017	BG-PV-WT-BSS-Grid	Yes	No	Load	No	China
[57]-2017	BG-PV-Grid	Yes	No	Load (dairy farm)	No	-
[58]-2017	PV-ICE-BSS	Yes	No	DERs	No	-
[59]-2017	-	Yes	No	Load	No	-
[60]-2016	Diesel-PV-WT-BSS	Yes	No	Both	No	Eastern Cape South Africa
[61]-2016	Diesel-PV-BSS	Yes	Advanced	Load	No	Philippine/New Delhi, India
[62]-2011	diesel-WT-BSS-DR	No	Conventional	Load	No	-
Proposed	BG-PV-WT-BSS; BG-PV-SMES	Yes	Advanced	Both	Yes	Pakistan

TABLE 14. Salient features of urban vs rural MGs [63].

Features Detail	Urban MGs	Rural MGs
Density of area load (kW/km²)	500-100,000	2-50
Density of consumers (connection/km²)	Greater than 500	1-75
No. of consumers per km MV/LV line length	Greater than 75	1-75
Consumption density (kWh/km²)	Greater than 2,000,000	5000-200,000
Total costs per kWh (US$)	0.1-0.15	Grid based: 0.12-0.50 Diesel based: 0.25-1.0 or more PV based home systems: 0.5-5.0
Investment costs/connection (US$) exclusing generation/transmission	Less than 500	500-7000s Average: 1200 Maximum: greater than 100,000
Social sustainability	Limited	Specific financial support and solutions required
Technical/Institutional sustainability	Large projects; often high power technologies on supply/demand side; reasonable load factor due to mixed load	Various technologies and small-scale applications; low load factors due to dominant domestic/agricultural load; intensive customer coordination required; high ratio of labour to capital
Socio-cultural sustainability	Seldom of importance	Important
Economic sustainability	More opportunities for profitable businesses	Limited opportunities for profitable businesses

8.99 kW PV, 3 kW WT, 6 kW BG, 5.66 kW power converter and 14 battery units with 2.37 kWh rating for each unit. Second, a novel EMS is suggested for the rural microgrids in which control of power converter is developed with FCS-MPC and FOSMC. Simplified EMS also coordinates with other conventional controllers, which are designed for practical distributed energy resources (DERs) in rural hybrid MGs during priority load requirements and availability of renewable energy resources (RERs) for the priority load. The applied novel EMS is validated with improved outcomes fluctuating energy resources. FCS-MPC and FOSMC based coordinated controllers are implemented for a standalone BG-PV-SMES system with enhanced power quality. The suggested FOSMC and FCS-MPC based strategies take less rise and fall time intervals during disturbances of DC voltage. The suggested methodologies improved the load voltage and fully tracked the reference value of the voltage with no steady-state error under stable system operations. For the regulation of voltage, the suggested FOSMC and FCS-MPC schemes ensured enhanced power quality during steady state and transient conditions. Novel EMS and LPO with SMES is analyzed under the unbalanced loads. PI control is employed for the extraction of the maximum solar PV power with regulated DC voltage. Load power observer (LPO) scheme is suggested for the enhancement of the solar PV generation capacities for an islanded rural microgrid in order to reduce the sizes of the storage unit that will finally reduce the system cost. FLC is used for tracking the speed of the VSBG in order to gradually reduce the generator output power for the prevention of over-speeding during storage of extra energy in SMES. Moreover, PI, FOSMC and FCS-MPC control strategies are investigated and analyzed for the control of the power

converter. Lower harmonics in voltage with enhanced power quality is obtained. FOSMC and FCS-MPC controls for the rural microgrid design shows much higher performance as compared to PI controller (for instance, smooth power with THDs of only 2.21% and 2.03% compared to 4.92% for PI control. Moreover, experimental results of FOSMC and PI are compared. Future work include comparison of experimental results of FCS-MPC with FOSMC and PI under different conditions of RERs generations and loads.

APPENDIX A

From Table 13, it can be seen that very less work is done in the context of rural MGs in the entire world, especially in developing countries.

APPENDIX B

Table 14 shows the main differences between urban MGs and rural MGs in developing countries. Apart from other differences, it can be seen that the major difference between urban and rural MG is the power density per km^2.

REFERENCES

[1] S. M. Bhagavathy and G. Pillai, "PV microgrid design for rural electrification," *Designs*, vol. 2, no. 3, p. 33, Sep. 2018.
[2] K. Tazi, M. F. Abbou, and F. Abdi, *Performance Analysis of Micro-Grid Designs With Local PMSG Wind Turbines*. Berlin, Germany: Springer, 2019.
[3] S. Mittlefehldt, "From appropriate technology to the clean energy economy: Renewable energy and environmental politics since the 1970s," *J. Environ. Stud. Sci.*, vol. 8, no. 2, pp. 212–219, Jun. 2018.
[4] Y. T. Wassie and M. S. Adaramola, "Potential environmental impacts of small-scale renewable energy technologies in East Africa: A systematic review of the evidence," *Renew. Sustain. Energy Rev.*, vol. 111, pp. 377–391, Sep. 2019.
[5] C. Ibeto and C. Ugwu, "Exhaust emissions from engines fuelled with petrol, diesel and their blends with biodiesel produced from waste cooking oil," *Polish J. Environ. Stud.*, vol. 28, no. 5, pp. 3197–3206, 2019.
[6] S. O. Giwa, C. N. Nwaokocha, and H. O. Adeyemi, "Noise and emission characterization of off-grid diesel-powered generators in Nigeria," *Manage. Environ. Qual., Int. J.*, vol. 30, no. 4, pp. 783–802, Jun. 2019.
[7] M. Vaccari, G. M. Mancuso, J. Riccardi, M. Cantù, and G. Pannocchia, "A sequential linear programming algorithm for economic optimization of hybrid renewable energy systems," *J. Process Control*, vol. 74, pp. 189–201, Feb. 2019.
[8] S. Vendoti, M. Muralidhar, and R. Kiranmayi, "GA based optimization of an stand-alone hybrid renewable energy system for electrification in a cluster of villages in India," in *Proc. 5th Int. Conf. Sci. Technol. Eng. Math. (ICONSTEM)*, Mar. 2019, pp. 319–324.
[9] K. Lee and D. Kum, "The impact of energy dispatch strategy on design optimization of hybrid renewable energy systems," in *Proc. IEEE Milan PowerTech*, Jun. 2019, pp. 1–6.
[10] B. Zhou, D. Xu, C. Li, C. Y. Chung, Y. Cao, K. W. Chan, and Q. Wu, "Optimal scheduling of biogas–solar–wind renewable portfolio for multicarrier energy supplies," *IEEE Trans. Power Syst.*, vol. 33, no. 6, pp. 6229–6239, Nov. 2018.
[11] L. Bartolucci, S. Cordiner, V. Mulone, and M. Santarelli, "Short-therm forecasting method to improve the performance of a model predictive control strategy for a residential hybrid renewable energy system," *Energy*, vol. 172, pp. 997–1004, Jun. 2019.
[12] L. Bartolucci, S. Cordiner, V. Mulone, V. Rocco, and J. L. Rossi, "Renewable source penetration and microgrids: Effects of MILP–based control strategies," *Energy*, vol. 152, pp. 416–426, Jun. 2018.
[13] X. Chen, W. Wu, N. Gao, H. S.-H. Chung, M. Liserre, and F. Blaabjerg, "Finite control set model predictive control for LCL-filtered grid-tied inverter with minimum sensors," *IEEE Trans. Ind. Electron.*, vol. 67, no. 12, pp. 9980–9990, Dec. 2020.
[14] M. Novak, U. M. Nyman, T. Dragicevic, and F. Blaabjerg, "Analytical design and performance validation of finite set MPC regulated power converters," *IEEE Trans. Ind. Electron.*, vol. 66, no. 3, pp. 2004–2014, Mar. 2019.
[15] P. Falkowski and A. Sikorski, "Finite control set model predictive control for grid-connected AC–DC converters with LCL filter," *IEEE Trans. Ind. Electron.*, vol. 65, no. 4, pp. 2844–2852, Apr. 2018.
[16] J. Zou, W. Xu, J. Zhu, and Y. Liu, "Low-complexity finite control set model predictive control with current limit for linear induction machines," *IEEE Trans. Ind. Electron.*, vol. 65, no. 12, pp. 9243–9254, Dec. 2018.
[17] T. H. Nguyen and K.-H. Kim, "Finite control set–model predictive control with modulation to mitigate harmonic component in output current for a grid-connected inverter under distorted grid conditions," *Energies*, vol. 10, no. 7, p. 907, Jul. 2017.
[18] X. Su, M. Han, J. Guerrero, and H. Sun, "Microgrid stability controller based on adaptive robust total SMC," *Energies*, vol. 8, no. 3, pp. 1784–1801, Mar. 2015.
[19] Y. M. Alsmadi, E. Vidal-Idiarte, L. Martinez-Salamero, A. Alqahtani, R. Giral, V. Utkin, L. Xu, and A. Y. Abdelaziz, "Sliding mode control of photovoltaic based power generation systems for microgrid applications," *Int. J. Control*, vol. 93, pp. 1–12, Jan. 2020, doi: 10.1080/00207179.2019.1664762.
[20] C. A. Monje, Y. Chen, B. M. Vinagre, D. Xue, and V. Feliu-Batlle, *Fractional-Order Systems And Controls: Fundamentals and Applications*. Berlin, Germany: Springer, 2010.
[21] S. S. Majidabad, H. T. Shandiz, and A. Hajizadeh, "Nonlinear fractional-order power system stabilizer for multi-machine power systems based on sliding mode technique," *Int. J. Robust Nonlinear Control*, vol. 25, no. 10, pp. 1548–1568, Jul. 2015.
[22] H. U. R. Habib, S. Wang, M. R. Elkadeem, and M. F. Elmorshedy, "Design optimization and model predictive control of a standalone hybrid renewable energy system: A case study on a small residential load in Pakistan," *IEEE Access*, vol. 7, pp. 117369–117390, Aug. 2019.
[23] A. Waqar, M. S. Nawaz, M. Aamir, I. Alam, S. U. Ali, and J. Ahmad, "Multi-objective analysis of DER sizing in microgrids using probabilistic modeling," in *Proc. Int. Conf. Electr., Commun., Comput. Eng. (ICECCE)*, Jul. 2019, pp. 1–6.
[24] S. Rehman, H. U. R. Habib, S. Wang, M. S. Buker, L. M. Alhems, and H. Z. A. Garni, "Optimal design and model predictive control of standalone HRES: A real case study for residential demand side management," *IEEE Access*, vol. 8, pp. 29767–29814, 2020.
[25] O. Krishan and S. Suhag, "Techno-economic analysis of a hybrid renewable energy system for an energy poor rural community," *J. Energy Storage*, vol. 23, pp. 305–319, Jun. 2019.
[26] F. Diab, H. Lan, L. Zhang, and S. Ali, "An environmentally-friendly tourist village in Egypt based on a hybrid renewable energy system—-Part two: A net zero energy tourist village," *Energies*, vol. 8, no. 7, pp. 6945–6961, Jul. 2015.
[27] H. Fontenot and B. Dong, "Modeling and control of building-integrated microgrids for optimal energy management—A review," *Appl. Energy*, vol. 254, Nov. 2019, Art. no. 113689.
[28] M. S. Kumari and S. Maheswarapu, "Enhanced genetic algorithm based computation technique for multi-objective optimal power flow solution," *Int. J. Electr. Power Energy Syst.*, vol. 32, no. 6, pp. 736–742, Jul. 2010.
[29] J. B. Hmida, M. J. Morshed, J. Lee, and T. Chambers, "Hybrid imperialist competitive and grey wolf algorithm to solve multiobjective optimal power flow with wind and solar units," *Energies*, vol. 11, no. 11, p. 2891, Oct. 2018.
[30] C. Chen, J. Wang, Y. Heo, and S. Kishore, "MPC-based appliance scheduling for residential building energy management controller," *IEEE Trans. Smart Grid*, vol. 4, no. 3, pp. 1401–1410, Sep. 2013.
[31] H. U. R. Habib, S. Wang, B. S. Farhan, H. W. Salih, A. Waqar, and K. M. Kotb, "Load power smoothing and DC bus voltage control of PV-SMES standalone microgrid based variable speed DG using FLC-MPC approach," in *Proc. 3rd Int. Conf. Energy Conservation Efficiency (ICECE)*, Oct. 2019, pp. 1–6.
[32] L. Bartolucci, S. Cordiner, V. Mulone, V. Rocco, and J. L. Rossi, "Renewable source penetration and microgrids: Effects of MILP—Based control strategies," *Energy*, vol. 152, pp. 416–426, Jun. 2018.
[33] L. Luo, L. Gao, and H. Fu, "The control and modeling of diesel generator set in electric propulsion ship," *Int. J. Inf. Technol. Comput. Sci.*, vol. 3, no. 2, pp. 31–37, Mar. 2011.

[34] W. U. K. Tareen, M. T. Dilbar, M. Farhan, M. A. Nawaz, A. W. Durrani, K. A. Memon, S. Mekhilef, M. Seyedmahmoudian, B. Horan, M. Amir, and M. Aamir, "Present status and potential of biomass energy in Pakistan based on existing and future renewable resources," *Sustainability*, vol. 12, no. 1, p. 249, 2020, doi: 10.3390/su12010249.

[35] S. U. Din, Q. Khan, F. U. Rehman, and R. Akmeliawanti, "A comparative experimental study of robust sliding mode control strategies for underactuated systems," *IEEE Access*, vol. 6, pp. 1927–1939, 2018.

[36] T. Ahmed *et al.*, "Energy management of a battery storage and D-STATCOM integrated power system using fractional order sliding mode control," *CSEE J. Power Energy Syst.*, pp. 1–14, Oct. 2020, doi: 10.17775/CSEEJPES.2020.02530.

[37] K. Murugaperumal, S. Srinivasn, and G. R. K. D. Satya Prasad, "Optimum design of hybrid renewable energy system through load forecasting and different operating strategies for rural electrification," *Sustain. Energy Technol. Assessments*, vol. 37, Feb. 2020, Art. no. 100613.

[38] M. Ali, M. Aamir, H. S. Khan, A. Waqar, F. Haroon, and A. R. Jafri, "Lyapunov stability and performance analysis of the fractional order sliding mode control for a parallel connected UPS system under unbalanced and nonlinear load conditions," *Energies*, vol. 11, no. 12, p. 3475, Dec. 2018.

[39] T. Orlowska-Kowalska, M. Dybkowski, and K. Szabat, "Adaptive sliding-mode neuro-fuzzy control of the two-mass induction motor drive without mechanical sensors," *IEEE Trans. Ind. Electron.*, vol. 57, no. 2, pp. 553–564, Feb. 2010.

[40] R. A. DeCarlo, S. H. Zak, and G. P. Matthews, "Variable structure control of nonlinear multivariable systems: A tutorial," *Proc. IEEE*, vol. 76, no. 3, pp. 212–232, Mar. 1988.

[41] M. Súri, T. A. Huld, E. D. Dunlop, and H. A. Ossenbrink. (2020). *Photovoltaic Geographical Information System (PVGIS) | EU Science Hub*. Accessed: Nov. 23, 2020. [Online]. Available: https://ec.europa.eu/jrc/en/pvgis

[42] M. A. Jirdehi, V. S. Tabar, S. Ghassemzadeh, and S. Tohidi, "Different aspects of microgrid management: A comprehensive review," *J. Energy Storage*, vol. 30, Aug. 2020, Art. no. 101457.

[43] P. Mattavelli, "An improved deadbeat control for UPS using disturbance observers," *IEEE Trans. Ind. Electron.*, vol. 52, no. 1, pp. 206–212, Feb. 2005.

[44] J. M. Guerrero, P. C. Loh, T.-L. Lee, and M. Chandorkar, "Advanced control architectures for intelligent microgrids—Part II: Power quality, energy storage, and AC/DC microgrids," *IEEE Trans. Ind. Electron.*, vol. 60, no. 4, pp. 1263–1270, Apr. 2013.

[45] J.-W. Jung, N. T.-T. Vu, D. Q. Dang, T. D. Do, Y.-S. Choi, and H. H. Choi, "A three-phase inverter for a standalone distributed generation system: Adaptive voltage control design and stability analysis," *IEEE Trans. Energy Convers.*, vol. 29, no. 1, pp. 46–56, Mar. 2014.

[46] H. S. Khan, M. Aamir, M. Ali, A. Waqar, S. U. Ali, and J. Imtiaz, "Finite control set model predictive control for parallel connected online UPS system under unbalanced and nonlinear loads," *Energies*, vol. 12, no. 4, pp. 1–20, 2019.

[47] M. Nauman and A. Hasan, "Efficient implicit model-predictive control of a three-phase inverter with an output LC filter," *IEEE Trans. Power Electron.*, vol. 31, no. 9, pp. 6075–6078, Sep. 2016.

[48] G. H. Philipo, Y. A. C. Jande, and T. Kivevele, "Demand-side management of solar microgrid operation: Effect of time-of-use pricing and incentives," *J. Renew. Energy*, vol. 2020, Jun. 2020, Art. no. 6956214.

[49] L. Guo, Z. Yang, Y. Wang, and H. Xu, "Research on multi-scenario variable parameter energy management strategy of rural community microgrid," *Appl. Sci.*, vol. 10, no. 8, p. 2730, 2020.

[50] F. Azeem, G. B. Narejo, and U. A. Shah, "Integration of renewable distributed generation with storage and demand side load management in rural islanded microgrid," *Energy Efficiency*, vol. 13, no. 8, pp. 217–235, 2020.

[51] Z. Liu, J. Yang, W. Jiang, C. Wei, P. Zhang, and J. Xu, "Research on optimized energy scheduling of rural microgrid," *Appl. Sci.*, vol. 9, no. 21, p. 4641, Oct. 2019.

[52] A. H. Hubble and T. S. Ustun, "Composition, placement, and economics of rural microgrids for ensuring sustainable development," *Sustain. Energy, Grids Netw.*, vol. 13, pp. 1–18, Mar. 2018.

[53] R. Morsali and R. Kowalczyk, "Demand response based day-ahead scheduling and battery sizing in microgrid management in rural areas," *IET Renew. Power Gener.*, vol. 12, no. 14, pp. 1651–1658, Oct. 2018.

[54] A. Kumar, Y. Deng, X. He, P. Kumar, and R. C. Bansal, "Energy management system controller for a rural microgrid," *J. Eng.*, vol. 2017, no. 13, pp. 834–839, Jan. 2017.

[55] O. Longe, N. Rao, F. Omowole, A. Oluwalami, and O. Oni, "A case study on off-grid microgrid for universal electricity access in the Eastern Cape of South Africa," *Int. J. Energy Eng.*, vol. 7, no. 2, pp. 55–63, 2017.

[56] Z. Xin, Z. Man, W. Weizhou, Y. Jianhua, and J. Tianjun, "Scheduling optimization for rural micro energy grid multi-energy flow based on improved crossbreeding particle swarm algorithm," (in Chinese), *Trans. Chin. Soc. Agricult. Eng.*, vol. 33, no. 11, pp. 157–164, Jun. 2017. [Online]. Available: http://www.tcsae.org, doi: 10.11975/j.issn.1002-6819.2017.11.020.

[57] R. Sharma and X. Zhang, "Optimal energy management of a rural microgrid system using multi-objective optimization," U.S. Patent 2013/0 024 014 A1, Jan. 24, 2013.

[58] S. Mazzola, C. Vergara, M. Astolfi, V. Li, I. Perez-Arriaga, and E. Macchi, "Assessing the value of forecast-based dispatch in the operation of off-grid rural microgrids," *Renew. Energy*, vol. 108, pp. 116–125, Aug. 2017.

[59] G. Prinsloo, A. Mammoli, and R. Dobson, "Customer domain supply and load coordination: A case for smart villages and transactive control in rural off-grid microgrids," *Energy*, vol. 135, pp. 430–441, Sep. 2017.

[60] Z. Xu, M. Nthontho, and S. Chowdhury, "Rural electrification implementation strategies through microgrid approach in South African context," *Int. J. Electr. Power Energy Syst.*, vol. 82, pp. 452–465, Nov. 2016.

[61] J. Sachs and O. Sawodny, "A two-stage model predictive control strategy for economic diesel-PV-battery island microgrid operation in rural areas," *IEEE Trans. Sustain. Energy*, vol. 7, no. 3, pp. 903–913, Jul. 2016.

[62] S. Lu, E. Marcelo, J. Chunlian, S. Nader, K. Karanjit, M. Ebony, D. Ruisheng, and Z. Yu, "Control strategies for distributed energy resources to maximize the use of wind power in rural microgrids," in *Proc. IEEE Power Energy Soc. Gen. Meeting*, Jul. 2011, pp. 1–8.

[63] A. Zomers, "The challenge of rural electrification," *Energy Sustain. Develop.*, vol. 7, no. 1, pp. 69–76, Mar. 2003.

HABIB UR RAHMAN HABIB (Member, IEEE) was born in Fort Abbas, Pakistan. He received the B.Sc. degree in electrical engineering and the M.Sc. degree in electrical power engineering from the University of Engineering and Technology Taxila, Pakistan, in 2009 and 2015, respectively. He is currently pursuing the Ph.D. degree with the State Key Laboratory of Advanced Electromagnetic Engineering and Technology, Huazhong University of Science and Technology, Wuhan, China. Since 2009, he has been with the COMSATS Institute of Information Technology, Pakistan, and the Wah Engineering College, University of Wah, Pakistan. He has been a Management Trainee Officer (Maintenance Department) with Dynamic Packaging Pvt. Ltd., Lahore, Pakistan. He is also permanently with the Department of Electrical Engineering, University of Engineering and Technology Taxila, Pakistan. His research interests include rural microgrids (MGs), sustainable development, renewable energy resources (RERs), optimal planning, energy management system (EMS), combined heat and power (CHP); vehicle to grid (V2G), model predictive control (MPC) and its Applications in Power Industry. He is a business development leader/ambassador, founder, chairman and CEO of SI multinational corporation to promote green energy access to everyone on the globe.

ASAD WAQAR received the degree in electrical engineering from UET Taxila, in 2002, the master's degree in electrical power engineering from RWTH Aachen, Germany, in 2011, and the Ph.D. degree in electrical engineering from the Huazhong University of Science and Technology, China, in 2016. He was with industry for several years. He is currently an Associate Professor with the Department of Electrical Engineering, Bahria University, Islamabad, Pakistan, where he is also a Coordinator with the Post Graduate Programs. His research interests include smart grids, microgrid operation and control, power quality, power electronics, and network reinforcement planning.

ABDUL KHALIQUE JUNEJO was born in Larkana, Sindh, Pakistan, in 1989. He received the bachelor's and master's degrees in electrical engineering from the Quaid-e-Awam University of Engineering, Science and Technology (UEST), Nawabshah, Pakistan, in 2011 and 2015, respectively, and the Ph.D. degree from the State Key Laboratory of Advanced Electromagnetic Engineering and Technology, School of Electrical and Electronic Engineering, Huazhong University of Science and Technology, Wuhan, China. Since January 2016, he has been working as an Assistant Professor with Quaid-e-Awam UEST, Nawabshah, Pakistan. His research interests include the sliding mode control, linear and nonlinear control methods, permanent magnet synchronous machines, and observer design.

MAHMOUD F. ELMORSHEDY (Member, IEEE) was born in Gharbeya, Egypt, in 1989. He received the B.Sc. and M.Sc. degrees in electrical engineering from Tanta University, Tanta, Egypt, in 2012 and 2016, respectively. He is currently pursuing the Ph.D. degree with the State Key Laboratory of Advanced Electromagnetic Engineering and Technology, Huazhong University of Science and Technology, Wuhan, China. He has been working as a Teaching Assistant with the Department of Electrical Power and Machines Engineering, Faculty of Engineering, Tanta University, since 2013, where in June 2016, he was promoted to the degree of Assistant Lecturer. His research interests include linear induction motor, predictive control, power electronics, and renewable energy.

SHAORONG WANG was born in 1960. He received the B.E. degree in electrical engineering from Zhejiang University, Hangzhou, China, in 1984, the M.E. degree in electrical engineering from North China Electric Power University (NCEPU), Baoding, China, in 1990, and the Ph.D. degree in electrical engineering from the Huazhong University of Science and Technology (HUST), Wuhan, China, in 2004. He is currently a Professor with the School of Electrical and Electronics Engineering, Huazhong University of Science and Technology (HUST), Wuhan, China. His research interests include smart grids, power system operation and control, wind power, renewable energy, distributed generation, power grid planning, active distribution networks, AI and big data applications in power systems, and robotic inspection in power systems.

MAHMUT SAMI BÜKER received the master's degree from the KTH Royal Institute of Technology, Sweden, in Project Management and Operational Development under Mechanical Engineering Program and the Ph.D. degree in sustainable energy technologies from the University of Nottingham, U.K. He is currently an Assistant Professor in the field of renewable energy technologies with Konya NEU University. He has worked on a number of projects on solar assisted heating and cooling systems and has strong experimental and simulation skills as well as comprehensive energy analysis techniques through performance assessment of various renewable energy technologies. He is currently the author or coauthor of over 20 scientific articles particularly in renowned journals. His main interest areas of research are low/zero carbon technologies for buildings, solar thermal and hybrid PV/T systems, solar-assisted heating and cooling applications, thermal comfort, thermal energy storage, enhanced heat transfer and thermodynamics.

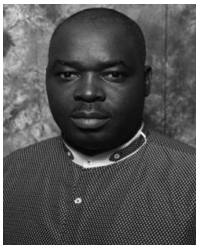

KAYODE TIMOTHY AKINDEJI (Member, IEEE) received the B.Sc. degree in electronic and electrical engineering and the M.Sc. degree in electronic and electrical engineering from Obafemi Awolowo University, Ile –Ife, Nigeria. He is currently pursuing the Ph.D. degree in electrical engineering from the University of Kwa-Zulu Natal (UKZN), Durban, South Africa. He also lectures at the Department of Electrical Power Engineering, Durban University of Technology (DUT). His research interests include smart grids, renewable energy, distributed generation, and micro-grid.

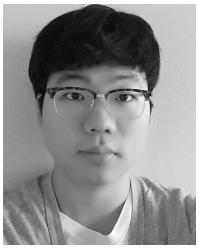

JEUK KANG was born in Seoul, South Korea, in 1996. He received the B.S. degree in electronic engineering from Hanyang University, Ansan, South Korea, in 2019. He is currently pursuing the Ph.D. degree with the Graduate School of Energy Convergence, Gwangju Institute of Science and Technology (GIST), Gwangju, South Korea.

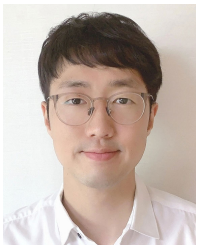

YUN-SU KIM (Member, IEEE) received the B.S. and Ph.D. degrees in electrical engineering from Seoul National University, Seoul, South Korea, in 2010 and 2016, respectively. He worked for the Korea Electrotechnology Research Institute (KERI) as a Senior Researcher from 2015 to 2017. He joined the Faculty of the Gwangju Institute of Science and Technology (GIST) in 2018, where he is currently an Assistant Professor with the Graduate School of Energy Convergence. He is the Director of the Korean Society for New and Renewable Energy and the Korean Institute of Electrical Engineers. His research interests include distribution networks, distributed energy resources, microgrid, artificial intelligence, and wireless power transfer.